Polymer Degradation and Stability xxx (2013) 1–17

Contents lists available at SciVerse ScienceDirect

Polymer Degradation and Stability

journal homepage: www.elsevier.com/locate/polydegstab

Novel cyclotriphosphazene-based epoxy compound and its application in halogen-free epoxy thermosetting systems: Synthesis, curing behaviors, and flame retardancy

Huan Liu, Xiaodong Wang*, Dezhen Wu

State Key Laboratory of Organic–Inorganic Composite Materials, School of Materials Science and Engineering, Beijing University of Chemical Technology, Beijing 100029, China

ARTICLE INFO

Article history:
Received 15 September 2012
Received in revised form
9 January 2013
Accepted 4 February 2013
Available online xxx

Keywords:
Cyclotriphosphazene-based epoxy compound
Synthesis
Thermosetting system
Curing kinetics
Flame retardancy

ABSTRACT

A novel cyclotriphosphazene-based epoxy compound (PN–EPC) as a halogen-free reactive-type flame retardant was synthesized via a two-step synthetic route. The chemical structures and compositions of the cyclotriphosphazene precursor and the final product were characterized by ^{1}H, ^{13}C, and ^{31}P NMR spectroscopy, Fourier transform infrared spectroscopy, mass spectroscopy, and elemental analysis. A series of thermosetting systems based on a conventional epoxy resin and PN–EPC were prepared, and their thermal curing behaviors were investigated. These epoxy thermosets achieved a significant improvement in glass transition temperature and also gained the good thermal stability with a high char yield. The incorporation of PN–EPC could impart an excellent nonflammability to the epoxy thermosets due to a synergistic flame retarding effect as a result of the unique combination of phosphorus and nitrogen from the phosphazene rings, and these epoxy thermosets achieved the high limiting oxygen indexes and the UL-94 V-0 rating when 20 wt.% of PN–EPC was added. The study on flame-retardant mechanism indicates that the pyrolysis products of phosphazene rings acted in both the condensed and gaseous phases to promote the formation of intumescent phosphorus-rich char on the surface of the epoxy thermosets. Such a char layer can supply a much better barrier for underlying thermosets to inhibit gaseous products from diffusing to the flame, to shield the surface of the thermosets from heat and air, and to prevent or slow down oxygen diffusion. As a result, the resulting epoxy thermosets obtained an excellent nonflammability.

1. Introduction

As a class of the most widely used materials in the fields of modern electronic and microelectronic industries, the high-performanced and flame-retardant epoxy resins have been attracting a great attention from both the scientific communities and industrial associations in past decades [1,2]. Although traditional brominated epoxy resins have been well developed to meet the considerable secure requirements in these areas, the existence of halogen elements is still an important environmental issue because of the generation of highly toxic and potentially carcinogenic substances during combustion [3,4]. These toxic brominated substances are very harmful to human health and also pose pollution problems when released into the environment [5]. Therefore, such a type of halogen-containing epoxy materials keeps away from the trend of green chemistry and sustainable development. Moreover, the manufacturers also need to identify ways to comply with legislation on environmental impact and sustainability. For example, the European Union proposed restricting the use of brominated flame retardants in electric and electronic fields [6,7], and simultaneously, the World Health Organization and the US Environmental Protection Agency also recommended exposure limits and risk assessment of halogenous compounds [8,9]. In this case, there is a strong interest in the development and utilization of more environmentally friendly epoxy resins with high performance and good fire resistance.

The scientific literature has reported very diverse and efficient strategies for improving the fire resistance of epoxy resins in a halogen-free way [10,11]. It is well understandable that there are two approaches to achieve flame retardancy in polymers like epoxy resins, i.e., by incorporating the 'additive-type' and the 'reactive-type' flame retardants [12]. The additive-type flame retardants, as widely used ones, are generally incorporated into polymers directly by physical means. This usually provides the most economical and effective way of imparting flame retardancy to commercial

* Corresponding author. Tel.: +86 10 6441 0145; fax: +86 10 6442 1693.
E-mail address: wangxdfox@yahoo.com.cn (X. Wang).

0141-3910/$ – see front matter © 2013 Elsevier Ltd. All rights reserved.
http://dx.doi.org/10.1016/j.polymdegradstab.2013.02.008

polymers. However, a variety of problems like poor compatibility, leaching, and deterioration in mechanical properties weaken their attraction [11]. The application of the reactive-type flame retardants involves either the synthesis of new and intrinsically flame retarding polymers or modification of existing polymers through copolymerization with a flame retarding unit either in the macromolecular backbone or as a pendent group [13]. It is no doubt that the simultaneous addition of phosphorus- and nitrogen-containing flame retardants is a very effective way to impart a good fire-resistant property to epoxy resins as a result of the synergistically flame retarding effect [14,15]. Because the organophosphorus molecules are efficient radical scavengers and flame quenching materials, and combustion processes are essentially exothermic free-radical reactions, so the existence of radical stabilizers impedes combustion by the quenching mechanism [16,17]. On the other hand, the nitrogen-containing moieties that release inert gaseous by-products to form a highly porous char that provides thermal insulation and prevents the combustion from spreading [18,19]. Nevertheless, there are still some problems that result in a limitation of their use in the electronic and microelectronic fields with a requirement of high performance. Major one of them is that the deterioration in thermal, electric and mechanical properties is unacceptable for the fabrication of electronic parts and devices [11]. Therefore, the reactive approach, i.e., the incorporation of chemical units containing phosphorus, or nitrogen, or both into the macromolecular backbone or side chains, is considered as a more effective route, whose main advantage is to impart permanent flame retardancy as well as maintain the original physical properties of epoxy resins in a better way [20–22]. There are lots of work reported on the molecular design and synthesis of flame retardant epoxy resins as well as a reactive flame-retardant additives by incorporating phosphorus-containing flame retarding units such as phosphine oxide, phosphates, and the other phosphorylated and phosphonylated derivatives [23–26]. However, these phosphorus-containing epoxy resins hardly gain high weight fraction of phosphorus, resulting in a low degree of flame retardancy.

The development of flame-retardant epoxy resins and corresponding additives often requires the understanding of the mechanisms from the phenomena that take place during combustion. Many studies have discovered that the intrinsical flame retardancy of a polymeric material depends primarily on the nature and chemical structure of the polymer concerned, its decomposition mode and the required level of fire safety, and also the global performances of the resulting material [10,11]. Currently, a great interest is focusing on the redesign of both the backbone and the side groups of epoxy resins with more highly flame retarding moieties like phosphazenes, particularly cyclotriphosphazenes [8,13,27–30]. Cyclotriphosphazenes have a characteristic ring structure consisting of alternating phosphorus and nitrogen atoms with two substituents attached to the phosphorus atoms, and therefore, they can offer the synergism of the phosphorus–nitrogen combination resulting in outstanding flame retardancy and autoextinguishability [31,32]. This great advantage is ascribed to its unique molecular framework based on alternating phosphorus and nitrogen atoms in a conjugative mode. Another great advantage is that its rich substitution chemistry at the phosphorus center provides a flexible synthetic methodology for preparation of cyclotriphosphazene-based compounds with various substituents, which allows us to obtain multifunctional reactive-type flame retardants with ease [33,34].

In this work, we designed and synthesized a novel cyclotriphosphazene-based epoxy compound as a reactive-type flame retardant for halogen-free epoxy thermosetting systems. In most cases, this cyclotriphosphazene-based epoxy compound can be synthesized from commercially available hexachlorocyclotriphosphazene ($N_3P_3Cl_6$) with a variety of substituents via a nucleophilic substitution [35,36]. The good reactivity of replaceable chlorine atoms linked to the phosphorus atoms of a phosphazene ring offers synthetic adaptability to introduce a large number of substituents with appropriate functionality, which can subsequently be transformed into desired synthetic precursors [37]. Therefore, the synthesis of the cyclotriphosphazene-based epoxy compound is expected to be feasible and facile. Furthermore, the incorporation of the cyclotriphosphazene-based epoxy compound is expected to enhance the thermal resistance, thermal stability, and most importantly, excellent fire resistance of the resulting conversional epoxy thermosetting systems. A complementary study on the curing behaviors and flammability characteristics of these epoxy thermosetting systems was also performed and described in the current article.

2. Experimental

2.1. Chemicals

Hexachlorocyclotriphosphazene (**1**) was purchased from Shanghai Yagu Chemical Co., Ltd., China. It was purified by recrystallization from *n*-heptane followed by a vacuum sublimation (60 °C and 0.05 mm Hg) before use. Bisphenol-A (**2**), glycidol (**4**), triethylamine (TEA), ethyl acetate (EA), acetone, hydrochloric acid (HCl), dichloromethane (CH_2Cl_2), tetrahydrofuran (THF), and *n*-hexane were purchased from Beijing Chemical Reagent Co., Ltd., China. THF was distilled from sodium benzophenone ketal prior to use, and the other chemicals and reagents were used as received. Diglycidyl ether of bisphenol A (DGEBA) was commercially supplied by Wuxi Resin Factory of BlueStar New Chemical Materials Co., Ltd. Dicyandiamide (DICY), 4,4′-Diamino-diphenylmethane (DDM), and methyl tetrahydrophthalic anhydride (MeTHPA) were selected as hardeners and were also purchased from Beijing Chemical Reagent Co., Ltd., China.

2.2. Synthesis and reactions

2.2.1. Synthesis of 2,2′-bis(4-oxo-penta-chloro-cyclotriphosphazene phenyl) propane (*3*)

A 500 mL three-necked round-bottom flask equipped with a reflux condenser, a nitrogen inlet, and a dropping funnel was charged with a solution of **1** (25 g, 0.07 mol) and TEA (5.8 g, 0.055 mol) in THF (200 mL). A solution of **2** (6.55 g, 0.029 mol) in THF (100 mL) was added dropwise into the flask over 2 h with agitation, followed by stirring for 24 h under a nitrogen atmosphere. After the reaction was completed, the reaction mixture was filtered and then washed repeatedly with deionized water. The organic layer separated was dried with anhydrous Na_2SO_4 and concentrated on a rotatory evaporator under reduced pressure, leaving a white solid. Ultimately, this white solid was further purified by column chromatography (silica gel, 20 vol.% of AEC/80 vol.% of *n*-hexane), and the removal of solvent gave a off-white solid of **3** (20.05 g, yield 82.4%). ^{31}P NMR ($CDCl_3$): $\delta = -0.72$ (s, 2P) and -13.33 ppm (s, 1P). ^{1}H NMR ($CDCl_3$): $\delta = 1.69$ (s, 6H), 7.02 (d, 4H) and 7.23 ppm (d, 4H). ^{13}C NMR ($CDCl_3$): $\delta = 29.78$ (s, 2C), 41.57 (s, 1C), 119.79 (s, 2C), 127.25 (s, 4C), 146.35 (s, 4C), and 147.72 ppm (s, 2C). MS: $m/z = 851$ $[M+1]^+$. Elemental anal. Found: C, 21.46; H, 1.62; Cl, 41.73; N, 9.76. Calcd for $C_{15}H_{14}Cl_{10}N_6O_2P_6$: C, 21.18; H, 1.66; Cl, 41.68; N, 9.88; O, 3.76; P, 21.85.

2.2.2. Synthesis of 2,2′-bis(4-oxo-penta-glycidol-cyclotriphosphazene phenyl) propane (*5*)

4 (57.9 g, 0.625 mol) and TEA (23.75 g, 0.235 mol) were dissolved in acetone (150 mL) in a round-bottom flask equipped with a dropping funnel and a magnetic stirring bar, and the reaction

Please cite this article in press as: Liu H, et al., Novel cyclotriphosphazene-based epoxy compound and its application in halogen-free epoxy thermosetting systems: Synthesis, curing behaviors, and flame retardancy, Polymer Degradation and Stability (2013), http://dx.doi.org/10.1016/j.polymdegradstab.2013.02.008

mixture was cooled with an ice bath. Sequently, a solution of **3** (20 g, 0.0235 mol) in acetone (100 mL) was added dropwise into the flask over 1 h, and then the reaction mixture was vigorously stirred at room temperature for 12 h under a nitrogen atmosphere. After the reaction was completed, the reaction mixture was filtered, washed repeatedly with hot water, and then dried with anhydrous Na_2SO_4. The solvent was removed by rotatory evaporation under reduced pressure, and the final product afforded a dark brown solid of **5** (26.1 g, yield 90.6%) as the cyclotriphosphazene-based epoxy compound we targeted. 31P NMR ($CDCl_3$): $\delta = -0.95$ (s, 2P) and −13.26 ppm (s, 2P). 1H NMR ($CDCl_3$): $\delta = 1.66$ (s, 6H), 2.47 (m, 10H), 2.61 (d, 10H), 2.63 (s, 10H), 3.43–3.76 (m, 20H), 6.86 (d, 4H) and 7.15 ppm (s, 4H). 13C NMR ($CDCl_3$): $\delta = 29.85$ (s, 2C), 41.42 (s, 1C), 44.88 (s, 10C), 52.86 (s, 10C), 56.01 (s, 10C), 119.71 (s, 2C), 127.18 (s, 4C), 146.85 (s, 4C), and 147.54 ppm (s, 2C). MS: $m/z = 1227.25$ $[M+1]^+$, Elemental anal. Found: C, 43.87; H, 5.21; N, 6.89. Calcd for $C_{45}H_{64}N_6O_{22}P_6$: C, 44.05; H, 5.26; N, 6.85; O, 28.69; P, 15.15.

2.3. Curing procedure of cyclotriphosphazene-based epoxy compound

A series of epoxy curing systems consisting of DGEBA and various amounts of **5** was cured using DICY, DDM, and MeTHPA as hardeners. DGEBA and **5** was dissolved in appropriate amount of acetone, and then the hardener was added with an equivalent ratio to the epoxy curing system of 1:1. 2,4,6-Tris(dimethylaminomethyl) phenol (0.2 wt.%) as a curing accelerator was also added into this solution. The mixture was stirred constantly to be a homogenous solution and then was kept in a vacuum oven at 90 °C for 3 h to remove the solvent. A two-step curing procedure was carried out in a mold to obtain the thermosetting resins. The epoxy formulations containing DICY, DDM, and MeTHPA, were first precured at 150 °C for 2 h, and then were further postcured at 180 for 3 h. At the end of the curing procedure, the cured systems were cooled gradually to room temperature to avoid stress crack.

2.4. Characterization

2.4.1. Nuclear magnetic resonance (NMR) spectroscopy

^1H, ^{13}C and ^{31}P NMR spectra of the synthesized cyclotriphosphazene-based precursors and final product targeted were obtained using a Bruker AV-400 400 MHz spectrometer in deuterochloroform ($CDCl_3$) solution, and were referenced to external tetramethylsilane (TMS) and 85% H_3PO_4 with positive shifts recorded downfield from the reference. The ^{13}C and ^{31}P NMR spectra were proton decoupled.

2.4.2. Elemental analysis

The elemental analysis was performed with a Vario–EL–cube CHNS elemental analyzer (Elementar Analysensysteme GmbH).

2.4.3. Fourier transform infrared (FTIR) spectroscopy

FTIR spectra were obtained using a Bruker Tensor-27 FTIR spectrometer with a scanning number of 50. A finely ground, approximately 1 wt.% mixture of a solid sample in KBr powders is fused into a transparent disk for FTIR measurement using a hydraulic press.

2.4.4. Epoxy equivalent weight measurement

The epoxy equivalent weight (EEW) of the synthesized CTP-EC was determined by the HCl/acetone chemical titration method.

2.4.5. Differential scanning calorimetry (DSC)

The thermal curing study of the epoxy resin with various hardeners was carried out on a TA Instruments Q20 differential scanning calorimeter equipped with a thermal analysis data station, operating at heating rates of 5, 10, 15, and 20 °C/min under a nitrogen atmosphere. Thermal transition temperatures were also determined by DSC measurement.

2.4.6. Thermogravimetric analysis (TGA)

TGA measurements were performed under a nitrogen atmosphere using a TA Instruments Q50 thermal gravimetric analyzer. The samples with a mass of about 10 mg were placed in an aluminum crucible, and ramped from room temperature up to about 800 °C at a heating rate of 10 °C/min, while the flow of nitrogen was maintained at 50 mL/min.

2.4.7. Limiting oxygen index test (LOI)

LOI tests were performed using an HD-2 oxygen index apparatus with a magneto-dynamic oxygen analyzer, according to the ASTM D-2863 standard. The mixture of oxygen and nitrogen gas was continuously sent through the combustion chamber at a flow rate of 170 mL/min. The sample bar with a dimension of 65 × 3.0 × 1.6 mm was clamped vertically in the holder in the center of the combustion column. The top of the sample bar was ignited using a butane gas burner so that the sample bar was well lit and the entire top was burning. The relative flammability of the sample bar was determined by measuring the minimum concentration of oxygen, which would just support flaming combustion of the sample bar.

2.4.8. UL-94 vertical burning test

UL-94 vertical burning experiments were carried out based on the testing method proposed by Underwriter Laboratory according to ASTM D-1356/2002 standard. Five test sample bars with a dimension of 127 × 12.7 × 1.6 mm suspended vertically over surgical cotton were ignited using a butane gas burner. The end of the sample bar was ignited twice, and each ignition was carried out for 10 s. The classification of V-0 is obtained if the burning time of each sample bar after 10-s ignition does not exceed 10 s, and the total burning time for five samples does not exceed 50 s; at the same time, the surgical cotton below the specimen cannot be ignited by the flaming drippings.

2.4.9. Scanning electronic microscopy (SEM)

The SEM observation was performed on a Hitachi S-4700 scanning electron microscope to investigate the morphologies of the residual chars. The char samples for SEM were obtained after combustion in the vertical burning tests and were made electrically conductive by sputter coating with a thin layer of gold–palladium alloy. The images were taken in a high vacuum mode with 20 kV acceleration voltage and in a medium spot size.

3. Results and discussion

3.1. Synthesis and characterization

The synthetic pathway and methodology of the cyclotriphosphazene-based epoxy compound were schematically described in Fig. 1, in which the structural features of the cyclotriphosphazene precursor and the targeted product were also clearly illustrated. This cyclotriphosphazene-based epoxy compound **5** could be synthesized by two-step substitution reactions. The cyclotriphosphazene precursor **3** was first synthesized by a geminal substitution reaction of **2** with a commercial product **1**. This synthetic route is straightforward in a good yield of the final product. The molecular structure of **3** was characterized by means of ^1H, ^{13}C, and ^{31}P NMR spectroscopy and FTIR spectroscopy. As shown by Fig. 2, the ^{31}P NMR spectrum of **3** exhibits a total of two

Please cite this article in press as: Liu H, et al., Novel cyclotriphosphazene-based epoxy compound and its application in halogen-free epoxy thermosetting systems: Synthesis, curing behaviors, and flame retardancy, Polymer Degradation and Stability (2013), http://dx.doi.org/10.1016/j.polymdegradstab.2013.02.008

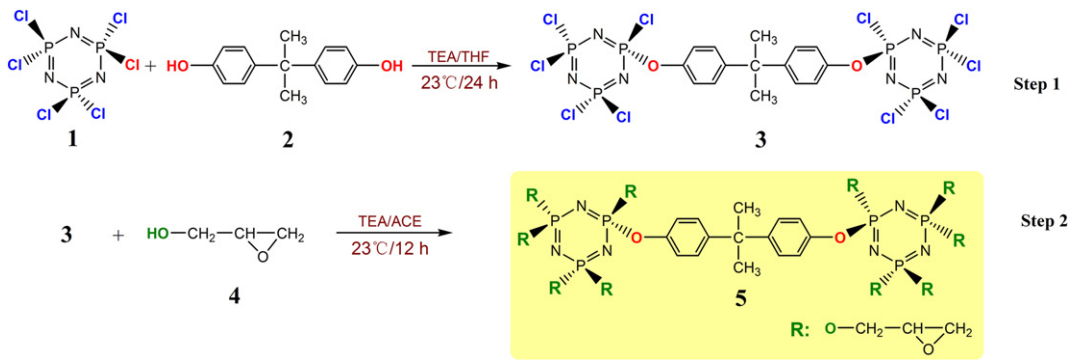

Fig. 1. Scheme of the synthetic route for cyclotriphosphazene-based epoxy compound (PN–EPC).

sets of singlet resonance signals, while the spectrum of **1** as a reference only shows an intensive singlet resonance signal at $\delta = -0.79$ ppm. The different chemical environments at the phosphorus centers for **3** result in a singlet signal at $\delta = -13.33$ ppm assigned to the monosubstituted phosphorus atom and another singlet one at $\delta = -0.79$ ppm for the other two phosphorus atoms bearing four chloride atoms in the proton-decoupled ^{31}P NMR spectrum. These two different environmental phosphorus atoms, i.e., (P*–OCl) and (P*–Cl_2), give an integration ratio of 1:2. The ^{1}H spectrum of **3** presented in Fig. 3 shows an intensive singlet resonance signal at $\delta = 1.69$ ppm, which is assigned to six methylic protons ($-CH_3^*$). Furthermore, the other two sets of doublet resonance signals are observed at 7.3–6.6 ppm corresponding to eight aromatic protons, whose assignments are explicated in the inserted spectrum of Fig. 3. The ^{13}C NMR spectrum also confirms the structure of **3** by the well-assigned locations of carbon atoms as presented in Fig. 4. Fig. 5 shows the FTIR spectrum of **3**, which clearly displays the appearance of absorption peak at 951 and 1172 cm^{-1} representing the formation of P–O–C bond due to the substitution reaction between **1** and **2**. Meanwhile, a characteristic P–N stretching bond at 1105 cm^{-1} and a strong P=N stretching vibration in the infrared spectrum at 1210–1290 cm^{-1} confirm the presence of phosphazene ring. The characteristic absorption peaks corresponding to the aromatic C–H of phenoxy groups are

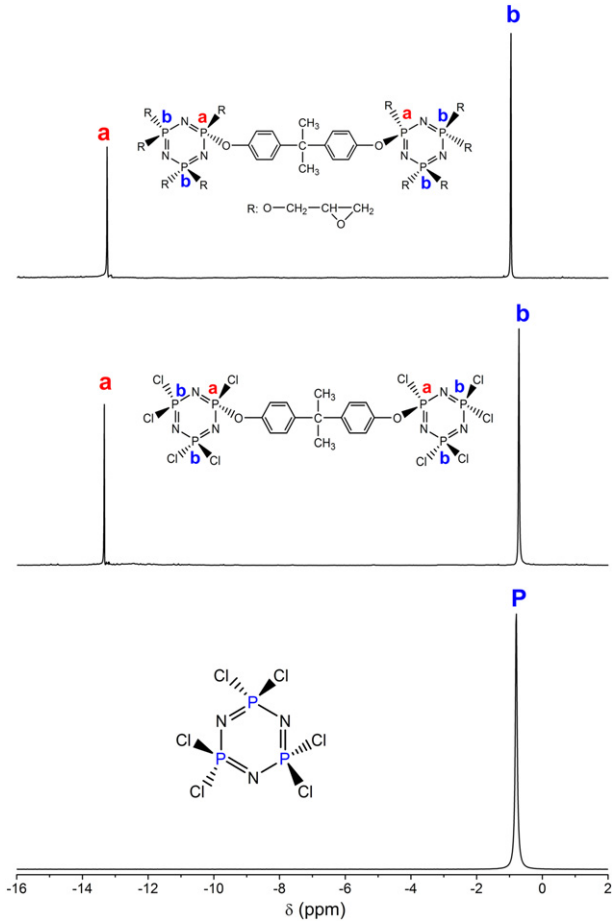

Fig. 2. ^{31}P NMR spectrum of cyclotriphosphazene precursor and PN–EPC.

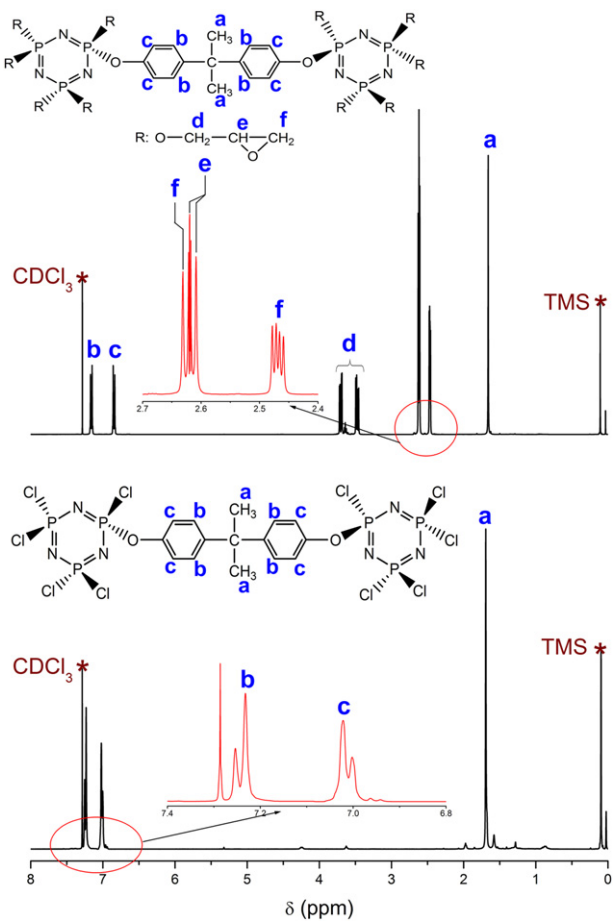

Fig. 3. ^{1}H NMR spectrum of cyclotriphosphazene precursor and PN–EPC.

Please cite this article in press as: Liu H, et al., Novel cyclotriphosphazene-based epoxy compound and its application in halogen-free epoxy thermosetting systems: Synthesis, curing behaviors, and flame retardancy, Polymer Degradation and Stability (2013), http://dx.doi.org/10.1016/j.polymdegradstab.2013.02.008

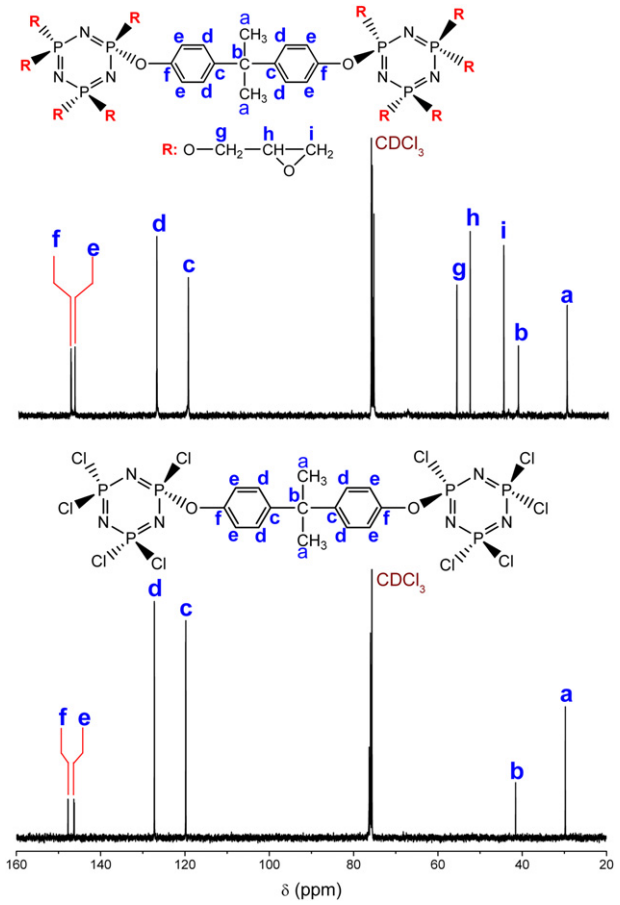

Fig. 4. ^{13}C NMR spectrum of cyclotriphosphazene precursor and PN–EPC.

observed at 3066, 1596, 1477, 762, and 689 cm^{-1}. These characterization data indicate that the cyclotriphosphazene precursor **3** has been successfully synthesized, and no side products are detected. In addition, the mass spectrum shows M^+ at *m/z* 850 consistent with the chemical structure of **3**, and the element analysis data also confirm the various element ratios in **3**.

The cyclotriphosphazene precursor **3** was conveniently reacted with **4** to complete the full substitution of chloride atoms in its phosphazene ring so as to get the targeted product **5**. The chemical

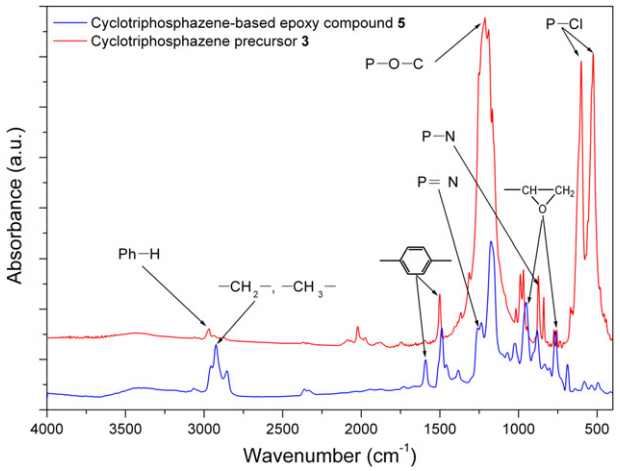

Fig. 5. FTIR spectrum of cyclotriphosphazene precursors and PN–EPC.

structure of **5** was also monitored by ^1H, ^{13}C, and ^{31}P NMR spectroscopy and FTIR spectroscopy. It is observed from Fig. 2 that ^{31}P NMR spectrum of **5** presents a similar pattern with that of **3**, where two set of singlet resonance signals appear at $\delta = -0.95$ and -13.26 ppm, corresponding to the two different environmental phosphorus atoms of cyclotriphosphazene, i.e., $P^*-(OC_6H_4)_2$ and $P^*-(OCH_2)(OC_6H_4)$, respectively. It is interesting to note that the resonance signal for the two phosphorus atoms geminally substituted with glycidol groups slightly shifted downfield from the location before substitution reaction. The ^1H NMR spectrum of **5** shows a several sets of resonance signals as shown by Fig. 3. Although there are several sets of complicated resonance signals, they are well assigned to all the protons of **5** as labeled and explicated in the inset of Fig. 3. As is shown by this spectrum, the resonance signals corresponding to the aromatic protons appear as two sets of doublets in the range of 7.2–6.8 ppm as a typical region for the benzene rings of both the substituents on cyclotriphosphazene and the backbone. A strong singlet resonance signal at 1.66 ppm is characteristic of the protons (labeled *a*) of methyl groups. Two sets of multiplet resonance signals at around 3.78–3.41 ppm corresponding to the protons (labeled *d*) of the methylene connected with *oxirane* rings are an indication of the reaction at these site to form the final epoxy resin. The other two sets of multiplet resonance signals at around 2.63 and 2.47 ppm are attributed to the protons (labeled *f*) of the methylene on *oxirane* ring, while a set of multiplet resonance signals appear at around 2.61 ppm as the assignment for the protons (labeled *e*) of methine on *oxirane* ring. Furthermore, as shown by Fig. 4, the ^{13}C NMR spectrum supports the chemical structure of **5** as well. The resonance signals for all the carbon atoms are in good agreement with expected chemical shifts for **5** and their assignments have been well labeled and depicted in Fig. 4.

The FTIR spectroscopy was also used to characterize the characteristic groups of **5**, and its spectrum was shown in Fig. 5. Two intensive absorption peaks can be observed at 1255 and 1231 cm^{-1} due to the asymmetrical N–P=N stretching, while an intensive bond corresponding to the symmetrical stretching vibration of P–N appears at 878 cm^{-1}, indicating the presence of the phosphazene rings. The characteristic peak at 1171 cm^{-1} is attributed to the P–O–C bonding. As an important feature of the spectrum, two distinct characteristic peaks of oxiranic C–O–C stretching vibration appear at 947 and 758 cm^{-1}. The absorption bands at 2923, 2869, and 1387 cm^{-1} are attributed to the stretching vibrations of $-CH_3$, $-CH_2-$, and $-C(CH_3)_2-$ groups, respectively. These results provide an evidence for the presence of the chemical groups of **5**. Additionally, the mass spectrum and elemental analysis results collected in experimental section are in good agreement with the data calculated in terms of the expected formula of **5**. These characterization results further confirm the chemical structure of **5**. The EEW of **5** has been determined by the HCl/acetone chemical titration method and shows a value of 628.74 g/equav. It is noteworthy that the EEW of this epoxy compound is very close to its theoretical values of 613.12 g/equav based on the MS result, indicating that the reaction between **3** and **4** performed completely.

3.2. Thermal curing behaviors and curing kinetics

The characterization of the curing behaviors of the thermosetting systems consisting of a conventional epoxy resin, DGEBA, and the cyclotriphosphazene-based epoxy compound, abbreviated to PN–EPC, were performed by dynamic DSC scans using DICY, DDM, and MeTHPA as hardeners. Herein, the exothermic peak temperature (T_p) was directly obtained from the dynamic scanning thermograms, and the curve integral was run to calculate the curing heat (ΔH) during overall curing process. Figs. 6–8 show the DSC

Please cite this article in press as: Liu H, et al., Novel cyclotriphosphazene-based epoxy compound and its application in halogen-free epoxy thermosetting systems: Synthesis, curing behaviors, and flame retardancy, Polymer Degradation and Stability (2013), http://dx.doi.org/10.1016/j.polymdegradstab.2013.02.008

thermograms of these thermosetting systems at various scanning rates, and corresponding data are summarized in Table 1. It is clearly observed that all the curing systems show a single exothermic peak corresponding to the curing reactions of the DGEBA/PN–EPC mixtures with hardeners, indicating that these curing reactions originated from a signal chemical process, and the thermal curing had been well performed for each curing system without any post-curing. As shown by these figures, the T_p for each sample of these three curing systems shifts to higher temperatures with the increase of scanning rate, which is a behavior widely described in the literature [38,39]. This phenomenon indicates that the curing reactions were accelerated by improving the curing temperature. It is interestingly observed that the DGEBA/PN–EPC thermosetting systems exhibit a different variation trend of the T_p with the PN–EPC content when using different hardeners. The DGEBA/PN–EPC thermosetting systems show slightly higher T_ps than the DGEBA ones either curing with DICY or with MeTHPA. In these two cases, the T_p increases with increasing the content of PN–EPC at a given heating rate. However, a contrary trend could be found for the curing systems with DDM. These results indicate that PN–EPC is less reactive than DGEBA when curing with DICY and with MeTHPA, but it is more reactive than DGEBA with DDM. It is also noted from Table 1 that the incorporation of PN–EPC results in a decrease of the ΔH for the curing systems with DDM, whereas the systems with DICY and MeTHPA present an opposite trend. This result confirms that the higher chemical reactivity of PN–EPC with DICY and MeTHPA.

The investigation of the curing kinetics of a new epoxy resins is important subject for the development and optimization of the curing cycles used in the manufacturing process of composite materials. Curing kinetic models can be used to simulate the curing process, and in this way, the cycle time can be minimized. The main objective of this work is to obtain the curing kinetic parameters of the thermosetting systems containing PN–EPC cured with various hardeners, because such parameters are necessary for the determination and optimization of the curing condition and thereby for the achievement of high performance of the corresponding thermosetting materials. The curing process of an epoxy thermosetting system is commonly described by a single step kinetic equation as follows:

$$\frac{d\alpha}{dt} = A\exp\left(-\frac{E}{RT}\right)f(\alpha) \tag{1}$$

where α represents the curing degree of an epoxy resin, T is the absolute temperature, t is the reaction time, A is the frequency factor, E is the activation energy of curing reaction, R is the gas constant, and $f(\alpha)$ is a model function that depends on the reaction mechanism. The curing kinetic models developed from kinetic analysis of DSC data have been widely applied to the curing reaction of epoxy resins [40,41]. Assuming the heat flow is proportional to the change in the extent of curing reaction:

$$\frac{d\alpha}{dt} = \frac{1}{\Delta H_0}\frac{dH}{dt} \tag{2}$$

where dH/dt represents the rate of heat generated during curing reaction, and ΔH_0 is the curing heat of overall curing reaction, which can be calculated by running the integral of curing dynamic DSC thermogram. There are several widely model-free kinetic

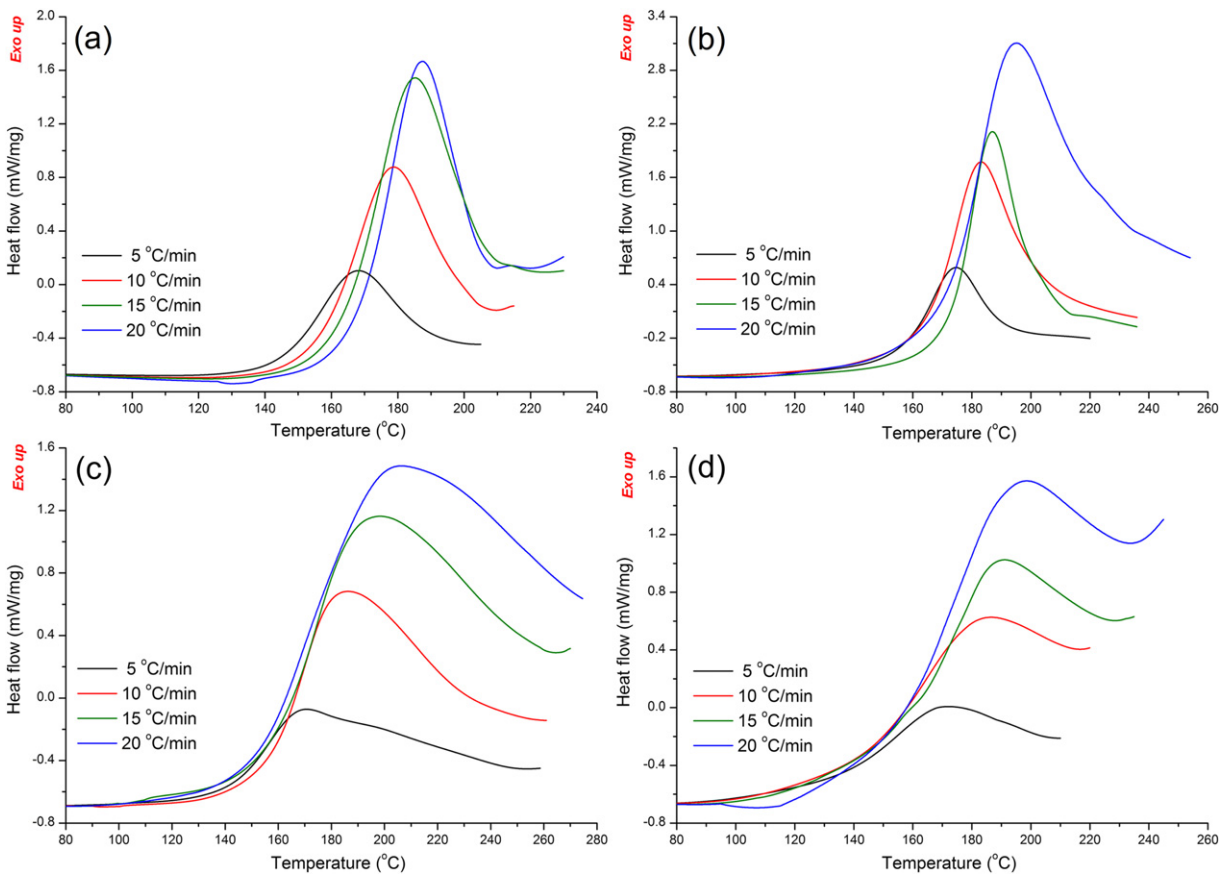

Fig. 6. Dynamic DSC scanning thermograms of the thermal curing reactions of epoxy mixtures with DICY at different scanning rates; (a) DGEBA, (b) DGEBA/5 wt.% PN-EPC, (c) DGEBA/10 wt.% PN-EPC, and (d) DGEBA/20 wt.% PN-EPC.

Please cite this article in press as: Liu H, et al., Novel cyclotriphosphazene-based epoxy compound and its application in halogen-free epoxy thermosetting systems: Synthesis, curing behaviors, and flame retardancy, Polymer Degradation and Stability (2013), http://dx.doi.org/10.1016/j.polymdegradstab.2013.02.008

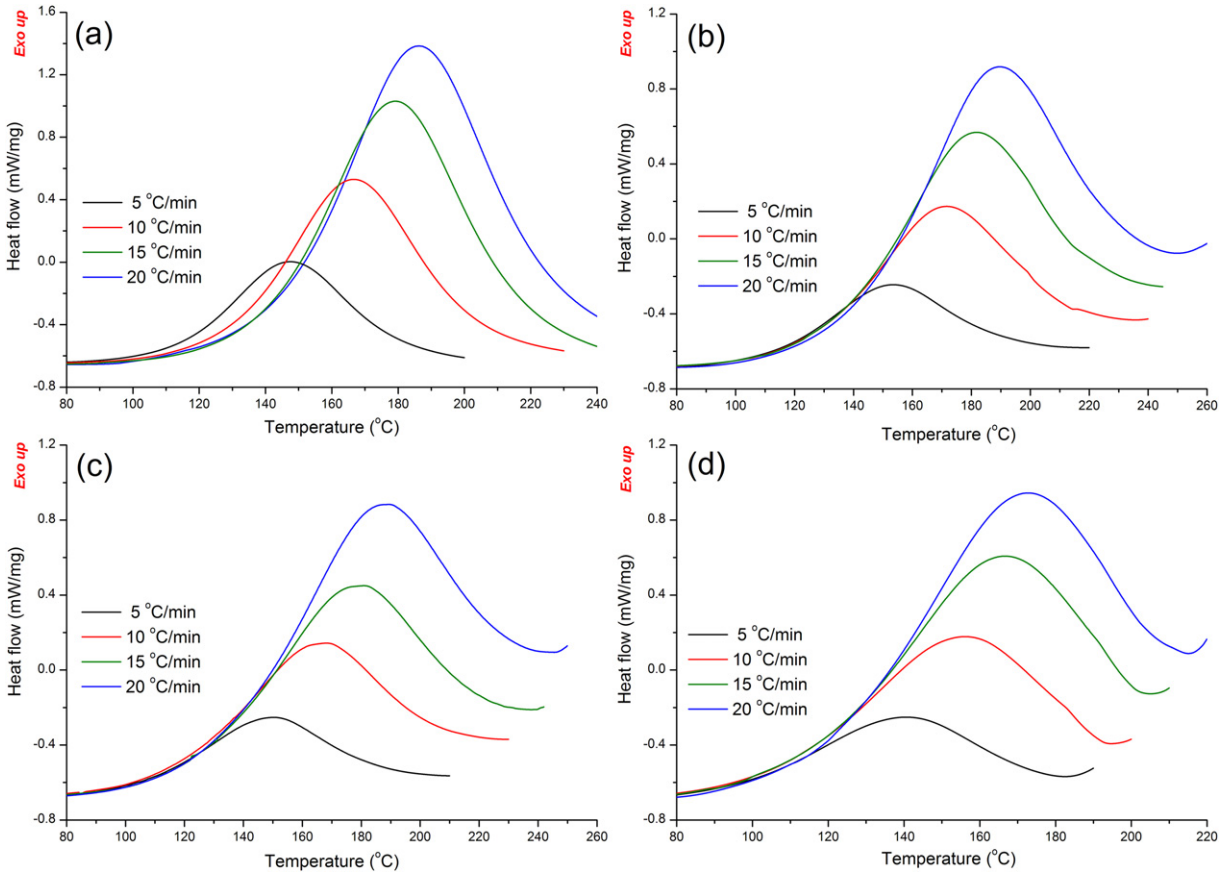

Fig. 7. Dynamic DSC scanning thermograms of the thermal curing reactions of epoxy mixtures with DDM at different scanning rates; (a) DGEBA, (b) DGEBA/5 wt.% PN-EPC, (c) DGEBA/10 wt.% PN-EPC, and (d) DGEBA/20 wt.% PN-EPC.

methods developed to estimate the parameters of the rate constant function (Eq. (1)). The well-known Kissinger–Akahira–Sunose (KAS) and Flynn–Wall–Ozawa (FWO) methods are frequently used to analyze the nonisothermal curing kinetics [42,43], since the kinetic parameters like E and A can be simply obtained from KAS's and FWO's equations without any assumption about the equation related to reaction conversion. In the case of KAS method, the activation energy (E_k) can be given from the slope of the plot of $\ln(\beta/T_p^2)$ versus $1/T_p$ by the equation as follows [44]:

$$-\ln\left(\frac{\beta}{T_p^2}\right) = \frac{E_k}{RT_p} - \ln\frac{AR}{E_k} \tag{3}$$

where β is the heating rate during dynamic scan. On the basis of the E_k obtained from the Kissinger–Akahira–Sunose (KAS) method, the Crane method gives a relationship between the β and the curing reaction order (n) and is expressed as follows [45]:

$$\frac{\mathrm{d}(\ln\beta)}{\mathrm{d}(1/T_p)} = -\left(\frac{E_k}{nR} + 2T_p\right) \tag{4}$$

As long as the $E_k/(nRT_p)$ is much greater than 2, the n can be derived from the slope of the plot of $\ln\beta$ versus $1/T_p$. Furthermore, the activation energy (E_o) derived from FWO method can also be obtained from the slope of the plot of $\ln\beta$ versus $1/T_p$ according to the FWO's equation expressed as follows [46]:

$$\ln\beta = -1.052\frac{E_o}{RT_p} + \ln\left(\frac{AE_o}{R}\right) - 5.331 \tag{5}$$

Figs. 9 and 10 illustrate the Kissinger and Ozawa plots for the DGEBA/PN–EPC curing systems with three hardeners, respectively. The curing kinetic parameters, i.e., E_k, E_o, n, and A, have been obtained from the slopes and intercepts of these plots and are summarized in Table 2. The data regarding the activation energy demonstrate a good agreement between Kissinger and Ozawa methods for these three curing systems. Although the activation energy of the thermosetting systems is variable due to the curing reactions with different hardeners, it is observed that the values of both E_k and E_o for the DGEBA curing systems exhibit a variation trendy in an order of DICY > MeTHPA > DDM. This result implies that the chemical reactivity of DGEBA with these three hardeners stands by an order of DDM > MeTHPA > DICY, which is in good agreement with the results of the T_ps. As is well known, the curing reaction of the epoxy group with an amine hardener is a typical nucleophilic substitution reaction, and the activation of oxirane-ring opening is mainly dependent on the proton donors during the course of reaction. The amine group has much stronger alkalinity than hydroxyl group, and the low steric hindrance of DDM can lead to a greater propensity towards nucleophilic attack in oxirane ring as well. Therefore, DDM is most reactive toward the oxirane ring among these three hardeners, which results in the lowest activation energy. The lower reactivity of DICY is probably due to an induction effect as a result of the decline in the nucleophilicity of nitrogen caused by the strong electron withdrawing cyano group on the DICY molecule. MeTHPA also exhibits a low chemical reactivity when curing with the epoxy thermosetting systems due to few proton donors, i.e., hydroxyl groups, generated during the course of reaction. As a result, these two hardeners show

Please cite this article in press as: Liu H, et al., Novel cyclotriphosphazene-based epoxy compound and its application in halogen-free epoxy thermosetting systems: Synthesis, curing behaviors, and flame retardancy, Polymer Degradation and Stability (2013), http://dx.doi.org/10.1016/j.polymdegradstab.2013.02.008

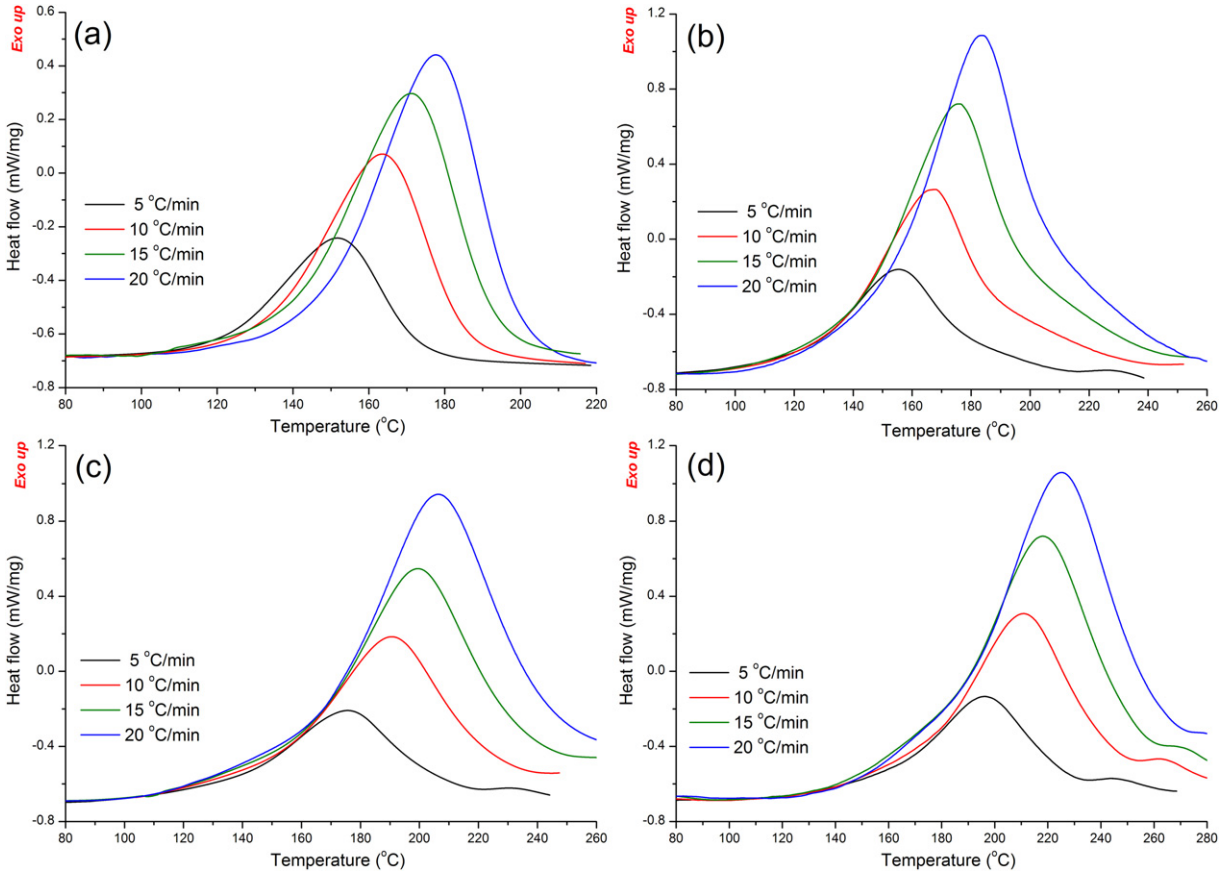

Fig. 8. Dynamic DSC scanning thermograms of the thermal curing reactions of epoxy mixtures with MeTHPA at different scanning rates; (a) DGEBA, (b) DGEBA/5 wt.% PN-EPC, (c) DGEBA/10 wt.% PN-EPC, and (d) DGEBA/20 wt.% PN-EPC.

the higher activation energy than DDM when curing with the epoxy resins.

Moreover, as is observed from the data listed in Table 1, it is important to point out that incorporating of PN–EPC also influenced the activation energy of these epoxy thermosetting systems due to the difference of chemical reactivity between DGEBA and PN–EPC. It is no doubt that the DGEBA/PN–EPC curing systems have the lower activation energy than DGEBA ones, since PN–EPC is more reactive toward three hardeners than DGEBA. However, the activation energy of DGEBA/PN–EPC curing systems exhibits an improvement with the continual increase of the PN–EPC content, and in some cases, it is higher than that of DGEBA ones. Apparently, compared to the bifunctional DGEBA, PN–EPC contains much more epoxy groups. Such a multifunctional feature generates a barrier for the curing reaction in the later curing stage due to the steric hindrance, constrains the mobility of crosslinked macromolecules, and consequently results in the high activation energy. In addition, it is interestingly observed from Table 1 that the reaction orders n of all the curing systems are similar and are all less than one, indicating that the curing process is complicatedly but follows the same

Table 1
The curing kinetic parameters obtained from DSC analysis for the curing reactions of the DGEBA/PN-EPC thermosetting systems with three hardeners.

Thermosetting system	5 °C/min		10 °C/min		15 °C/min		20 °C/min		Kissinger method			Ozawa method
	T_p (°C)	ΔH (J/g)	T_p (°C)	ΔH (J/g)	T_p (°C)	ΔH (J/g)	T_p (°C)	ΔH (J/g)	E_k (kJ/mol)	ln A (s^{-1})	n	E_o (kJ/mol)
DGEBA/DICY	168.57	210.8	179.14	196.8	185.17	162.3	187.37	123.1	112.51	29.55	0.94	114.07
DGEBA + 5 wt% PN-EPC[a]/DICY	173.57	217.8	183.50	239.8	190.86	254.6	203.28	158.4	75.01	18.83	0.91	78.60
DGEBA + 10 wt% PN-EPC[a]/DICY	174.79	218.0	182.59	254.4	186.88	271.6	205.07	341.7	75.57	29.51	0.94	77.19
DGEBA + 15 wt% PN-EPC[a]/DICY	172.98	235.6	184.69	259.4	194.53	285.2	204.17	251.8	64.47	15.91	0.89	68.54
DGEBA + 20 wt% PN-EPC[a]/DICY	175.09	228.3	184.73	245.4	191.09	131.9	207.85	127.0	80.08	20.31	0.91	83.32
DGEBA/DDM	147.72	327.0	166.82	260.0	179.75	344.2	186.20	355.7	62.43	12.34	0.87	65.93
DGEBA + 5 wt% PN-EPC[a]/DDM	153.98	220.8	172.81	224.8	183.27	218.1	189.26	202.5	56.10	14.09	0.88	60.34
DGEBA + 10 wt% PN-EPC[a]/DDM	153.34	213.2	168.14	228.8	180.67	188.8	187.43	178.2	52.32	13.12	0.88	56.71
DGEBA + 15 wt% PN-EPC[a]/DDM	154.62	218.2	163.61	258.2	172.27	173.3	176.22	174.0	61.23	15.99	0.89	65.06
DGEBA + 20 wt% PN-EPC[a]/DDM	141.35	204.4	157.82	196.5	167.89	174.3	174.04	162.6	57.54	15.09	0.89	61.49
DGEBA/MeTHPA	151.81	184.7	163.56	159.2	171.16	140.4	177.68	121.8	78.70	20.95	0.91	81.73
DGEBA + 5 wt% PN-EPC[a]/MeTHPA	156.34	283.0	167.99	264.7	176.40	261.5	184.43	255.7	73.96	19.33	0.91	77.30
DGEBA + 10 wt% PN-EPC[a]/MeTHPA	175.41	236.3	190.29	221.1	198.97	214.9	205.91	213.9	73.81	18.28	0.91	77.48
DGEBA + 15 wt% PN-EPC[a]/MeTHPA	195.93	244.6	210.66	234.2	217.58	233.9	224.79	227.0	86.46	20.72	0.92	89.82
DGEBA + 20 wt% PN-EPC[a]/MeTHPA	201.84	307.9	218.90	297.3	226.06	299.6	232.17	289.4	82.77	19.42	0.91	86.41

[a] The abbreviation of the cyclotriphosphazene-based epoxy compound.

Please cite this article in press as: Liu H, et al., Novel cyclotriphosphazene-based epoxy compound and its application in halogen-free epoxy thermosetting systems: Synthesis, curing behaviors, and flame retardancy, Polymer Degradation and Stability (2013), http://dx.doi.org/10.1016/j.polymdegradstab.2013.02.008

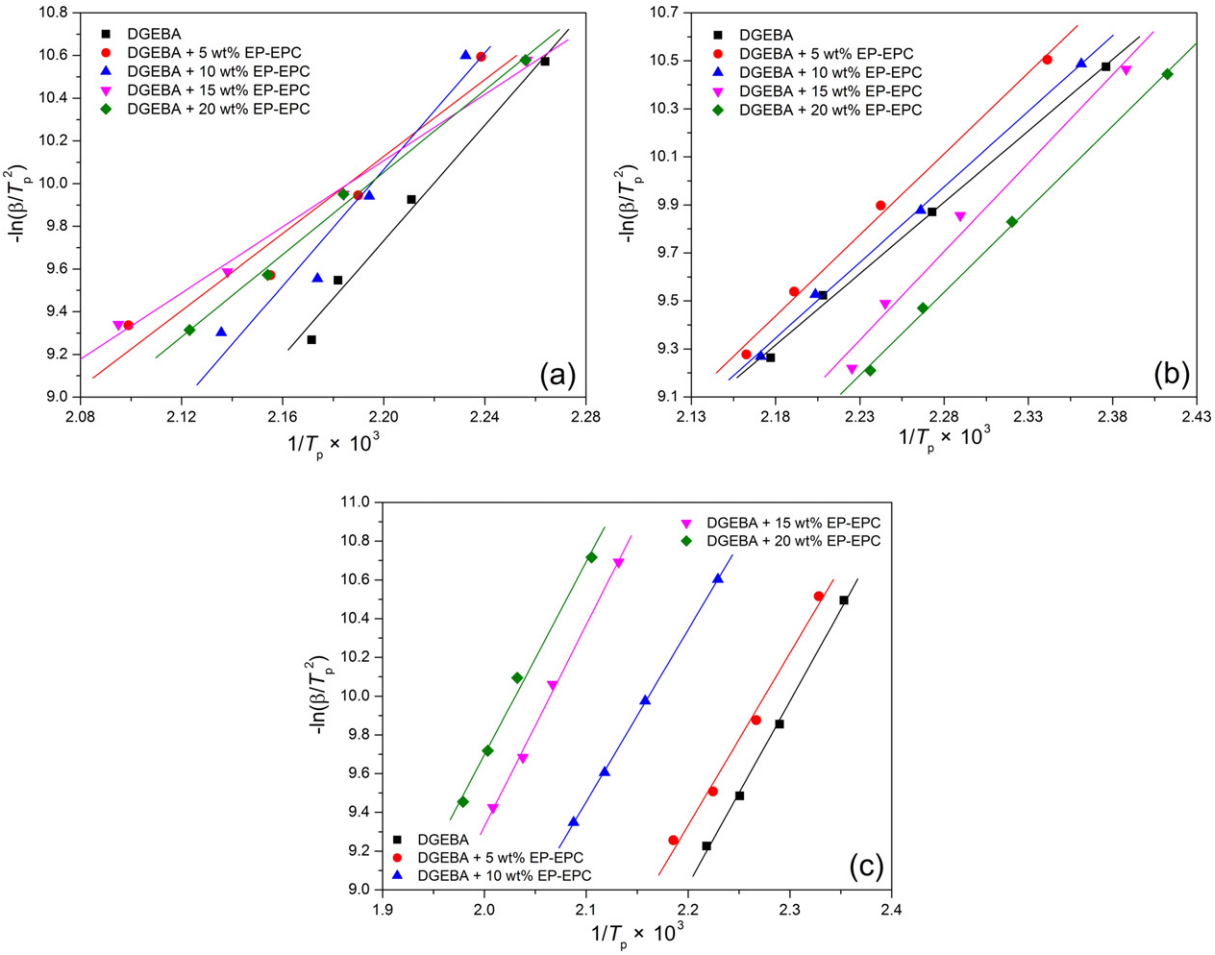

Fig. 9. The Kissinger's plots for the curing systems of DGEBA/PN–EPC mixtures with (a) DICY, (b) DDM, and (c) MeTHPA.

mechanism. However, the frequency factors *A* of these three curing systems show a strong dependence on the nature of hardeners. It is proposed that the higher values of the frequency factor for the curing systems with DICY and MeTHPA are attributed to the lower chemical reactivity toward the epoxy resins used in this study for the curing reaction. On the basis of the curing kinetic results obtained in this work, it is concluded that the these three hardeners are involved in the curing reaction with the DGEBA/PN–EPC mixtures in a different way and to a different extent, resulting in the different structural characteristics and physical properties of the resulting thermosetting materials.

3.3. Glass transition temperature

Glass transition temperature (T_g) is one of the most important parameters determining the thermal properties of an epoxy-based thermosetting material, because it establishes the service temperature for this material which are only used well, in most cases, at a temperature below T_g. Moreover, T_g is also a parameter which gives the information about the structure of crosslinked epoxy thermosets. Therefore, it is very important for the epoxy thermosetting materials to achieve a high T_g when designing the thermosetting systems. In this work, the T_gs of the DGEBA/PN–EPC thermosets cured with three hardeners were evaluated by DSC. Fig. 11 shows some reprehensive DSC traces selected from all the DSC thermograms, but all of the obtained results are summarized in Table 2. It is clearly seen that the DGEBA thermosets reveal a significant difference of T_g when cured with different hardeners. The thermosets with DICY and DDM exhibit a high T_g around 130 °C, and however, the one with MeTHPA has only a low T_g around 75 °C. It is generally agreed that the glass transition is generally ascribed to the segmental motion of the polymeric networks, and T_g is determined by the degree of freedom for the segmental motion, crosslinking and entanglement constraints, and the packing density of the macromolecular segments [40]. DICY and DDM are multifunctional curing agents, thus resulting in a high crosslinking degree. However, MeTHPA is only a bifunctional compound, which makes the cured thermosets a lower packing density and consequently results in a lower T_g.

It is surprisingly to find that the incorporation of PN–EPC significantly improved the T_gs of the thermosets cured either with DICY and DDM or with MeTHPA, and the T_gs of these thermosets strongly depended on the PN–EPC content. The higher the content of PN–EPC, the higher the T_g. Especially for the thermosets cured with MeTHPA, the T_g was increased to 123.95 °C by incorporating 20 wt.% of PN–EPC. Such a notable improvement in T_g indicates that the PN–EPC synthesized in this study can impart an excellent thermal resistance to the epoxy thermosets. As was aforementioned, PN–EPC is a multifunctional compound containing ten *oxirane* rings. When such a highly functionalized epoxy compound was introduced into the DGEBA thermosetting systems, the crosslinking degree and packing density of the cured thermosets were undoubtedly improved. Since the thermal motion of network in glassy state is believed to correspond to the motion of

Please cite this article in press as: Liu H, et al., Novel cyclotriphosphazene-based epoxy compound and its application in halogen-free epoxy thermosetting systems: Synthesis, curing behaviors, and flame retardancy, Polymer Degradation and Stability (2013), http://dx.doi.org/10.1016/j.polymdegradstab.2013.02.008

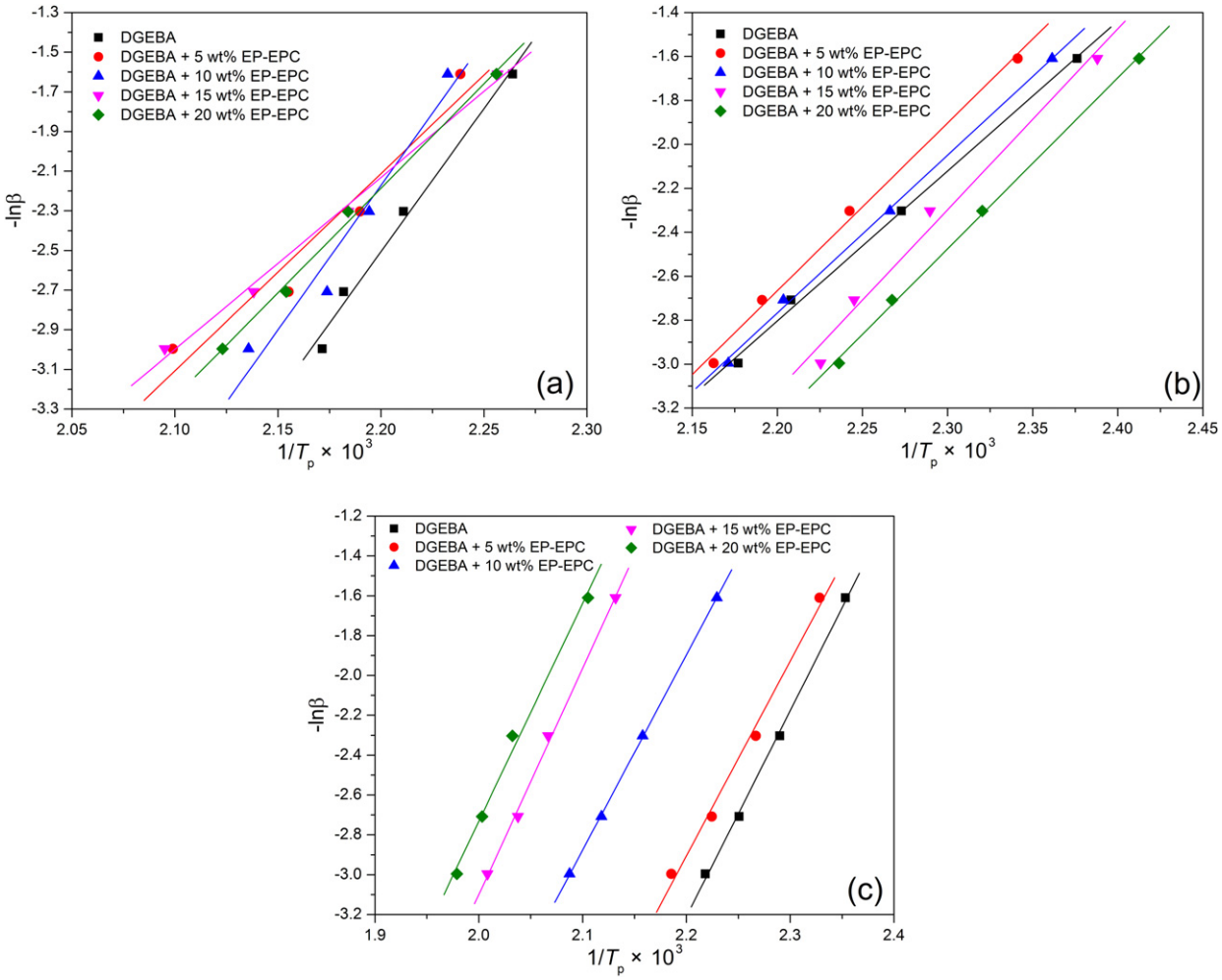

Fig. 10. The Ozawa's plots for the curing systems of DGEBA/PN–EPC mixtures with (a) DICY, (b) DDM, and (c) MeTHPA.

crosslinking segment, the high crosslinking degree and high packing density will shorten the molecular segments between two crosslinking points, and consequently reduce their mobility. Furthermore, the incorporation of the multifunctional PN–EPC also leads to a great steric hindrance and thus confines these motions. This effectively enhances the dimensional stability of the cured thermosetting systems at elevated temperature and thus improves the T_gs of DGEBA/PN–EPC thermosets.

Table 2
The thermal analysis results obtained from DSC and TGA measurements for the DGEBA/PN-EPC thermosets cured with three hardeners.

Thermoset sample	T_g (°C)	N_2 atmosphere			Air atmosphere		
		T_{onset}[b] (°C)	T_{max}[c] (°C)	Char yield at 750 °C (wt.%)	T_{onset}[b] (°C)	T_{max}[c] (°C)	Char yield at 750 °C (wt.%)
DGEBA/DICY	128.46	313.74	376.48	4.11	333.05	361.46	0.12
DGEBA+5 wt.% PN-EPC[a]/DICY	130.18	278.73	349.22	8.49	283.52	336.99	2.35
DGEBA+10 wt.% PN-EPC[a]/DICY	132.94	282.79	314.12	18.45	288.93	334.42	12.24
DGEBA+15 wt.% PN-EPC[a]/DICY	137.76	278.63	318.96	21.19	291.73	320.39	17.92
DGEBA+20 wt.% PN-EPC[a]/DICY	143.53	262.44	304.36	32.12	273.07	309.20	18.01
DGEBA/DDM	131.29	343.59	412.22	3.07	313.39	401.21	0.25
DGEBA+5 wt.% PN-EPC[a]/DDM	135.35	284.66	332.32	12.69	285.18	337.45	3.42
DGEBA+10 wt.% PN-EPC[a]/DDM	139.64	286.6	322.76	24.84	297.26	321.31	20.73
DGEBA+15 wt.% PN-EPC[a]/DDM	145.25	291.98	316.86	24.91	293.91	310.82	22.97
DGEBA+20 wt.% PN-EPC[a]/DDM	148.51	285.8	302.30	25.75	284.11	304.36	28.99
DGEBA/MeTHPA	74.62	302.49	415.33	3.24	279.66	406.76	0.13
DGEBA+5 wt.% PN-EPC[a]/MeTHPA	85.37	310.17	383.83	11.88	313.05	375.47	1.4
DGEBA+10 wt.% PN-EPC[a]/MeTHPA	93.48	255.72	353.62	13.72	296.65	358.48	4.26
DGEBA+15 wt.% PN-EPC[a]/MeTHPA	114.28	243.74	337.38	20.47	251.28	338.93	10.9
DGEBA+20 wt.% PN-EPC[a]/MeTHPA	123.95	266.06	332.86	22.71	234.95	332.44	15.04

[a] The abbreviation of the cyclotriphosphazene-based epoxy compound.
[b] The onset decomposition temperature, at which the thermoset undergoes 5 wt.% of weight loss.
[c] The characteristic temperature, at which maximum rate of weight loss occurs.

Please cite this article in press as: Liu H, et al., Novel cyclotriphosphazene-based epoxy compound and its application in halogen-free epoxy thermosetting systems: Synthesis, curing behaviors, and flame retardancy, Polymer Degradation and Stability (2013), http://dx.doi.org/10.1016/j.polymdegradstab.2013.02.008

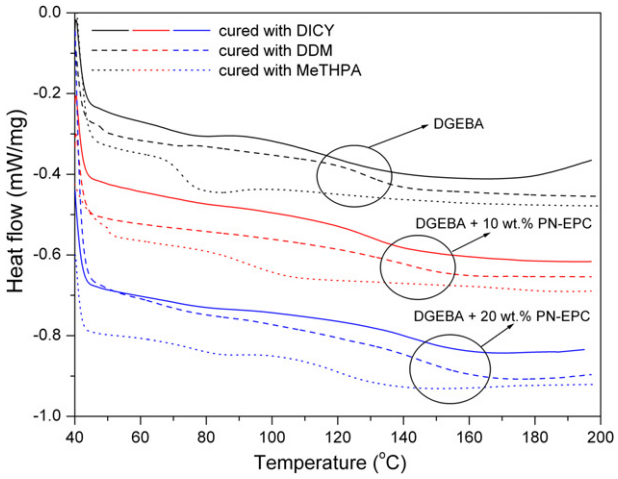

Fig. 11. DSC thermograms of DGEBA/PN–EPC thermosets cured with three hardeners.

3.4. Thermal stability

The effect of PN–EPC on the thermal stabilities of the epoxy thermosets cured with three hardeners was evaluated by TGA under both air and nitrogen atmospheres. Fig. 12 reveals the TGA thermograms of these thermosets, and the analysis results are summarized in Table 2. It is clearly observed from the TGA profiles that all of the thermosets present a typical one-stage degradation in air, whereas they exhibit a two-stage decomposition in nitrogen, which implies that, under different atmospheres, these epoxy thermosets underwent the decompositions in a different way for the major components of the polymeric networks. The temperature corresponding to 5 wt.% weight loss is defined as the onset decomposition temperature (T_{onset}) and furthermore taken as an indication of thermal stability. The TGA results show that the T_{onset}s of the DGEBA thermosets fall in the ranges of 305–345 °C in nitrogen and 279–333 °C in air. This indicates that the epoxy thermosets have a higher thermal stability in nitrogen than in air, since the oxygen in air can enhance the thermooxidative decomposition of the thermosets and thus accelerates the degradation. Meanwhile, the main degradation of these thermosets started at a maximum decomposition temperature (T_{max}) beyond 360 °C, at which the weight loss occurred at a maximum rate. And the thermosets also show slight higher T_{max}s in nitrogen than in air, which is consistent with the data of T_{onset}. These results indicate that the DGEBA thermosets cured with three hardeners have a good thermal stability in natural. It should be pointed out that the thermoset cured with DDM presents both a higher onset decomposition temperature and a higher maximum decomposition temperature than those with DICY and MeTHPA. This may be ascribed to the intrinsic chemical structure of the other two hardeners, which cannot endure a higher decomposition temperature.

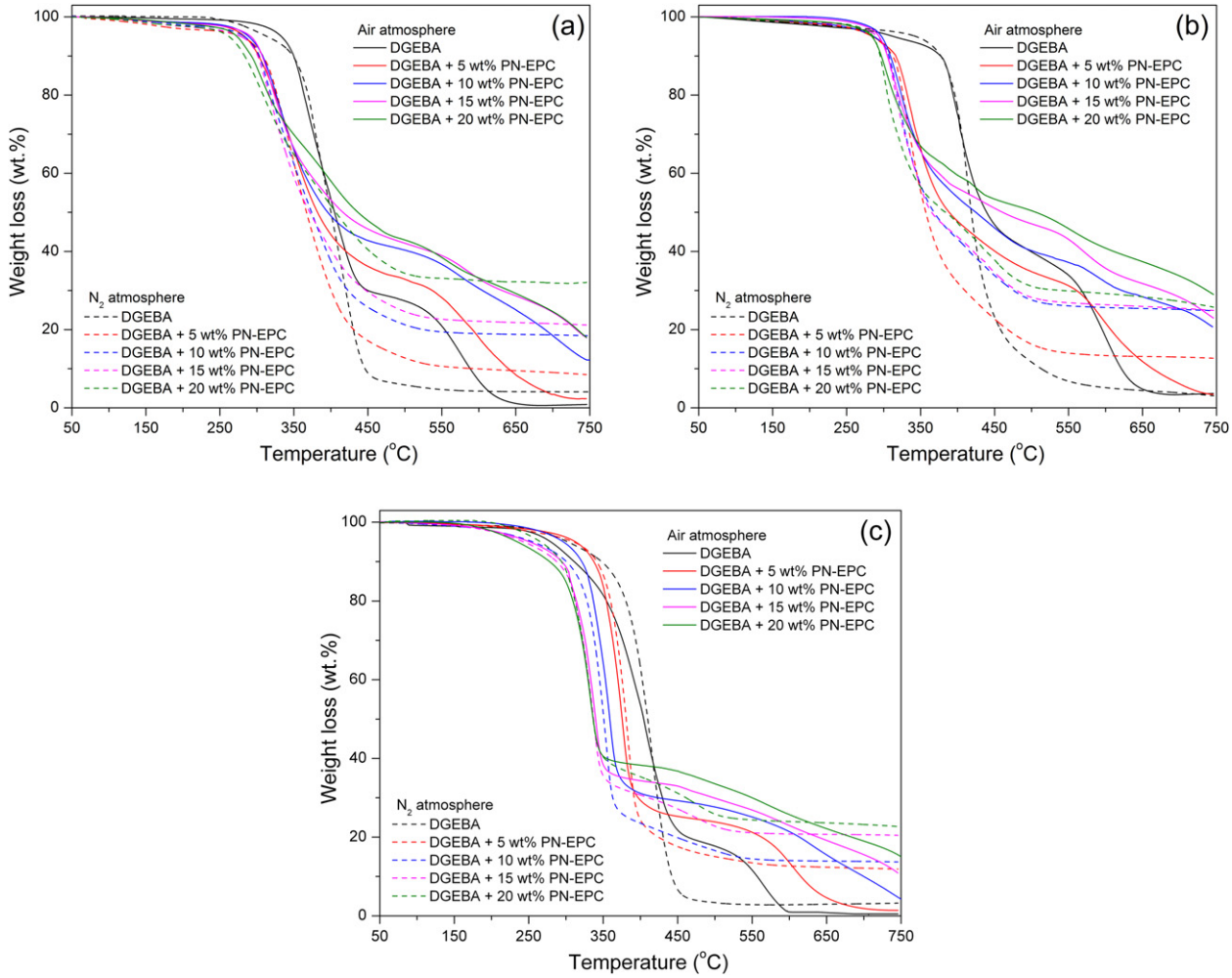

Fig. 12. TGA thermograms of DGEBA/PN–EPC thermosets cured with (a) DICY, (b) DDM, and (c) MeTHPA.

Please cite this article in press as: Liu H, et al., Novel cyclotriphosphazene-based epoxy compound and its application in halogen-free epoxy thermosetting systems: Synthesis, curing behaviors, and flame retardancy, Polymer Degradation and Stability (2013), http://dx.doi.org/10.1016/j.polymdegradstab.2013.02.008

As shown by the data in Table 2, all the DGEBA/PN–EPC thermosets show a reduction both in the T_{onset} and in the T_{max}, and the increase of the PN–EPC content leads to a further decrease in these two characteristic temperatures. This phenomenon indicates that the thermal stability of the epoxy thermosets decreased in the presence of PN–EPC, which may be ascribed to the less stable P–O–CH_2 bonds [12,47]. Although the DGEBA thermosets presented a completive degradation at 750 °C with a little char remained in nitrogen but almost with no char in air, the DGEBA/PN–EPC thermosets obtained high char yields at 750 °C, and the char yields also continuously increased with increasing the content of PN–EPC. Among these three thermosetting systems, thermoset cured with DICY obtained the highest char yields of 32.12 wt.% in nitrogen and 18.01 wt.% in air when 20 wt.% of PN–EPC was introduced. The thermosets cured with DDM and MeTHPA also achieved the high char yields more than 25 wt.% in nitrogen and 15 wt.% in air. The achievement of such a high char yield may be due to the highly thermally stable phosphazene rings in the thermosets. It is obvious that, when cyclotriphosphazene moieties is incorporated into the epoxy thermosetting systems in a covalent way, the phosphazene rings can undergo a highly crosslinking process to form a dense phosphorus-rich char during the thermal degradation and thus promotes the char formation of total thermosets [48,49]. Therefore, the further improvement in char yield can be gained by increasing the content of PN–EPC as a result of the increase in the number of phosphazene ring as well as in the content of phosphorus as a char-forming agent. It is also noted that the thermosets cured with DICY and DDM achieved higher char yield than those with MeTHPA both in nitrogen and in air. It is understandable that these two hardeners contain inert nitrogen elements, which can also enhance the char formation.

3.5. Flame-retardant property

The flame retardancy of the DGEBA/PN–EPC thermosets cured with three hardeners was investigated by the LOI and UL-94 vertical burning measurements, and the experimental results were collected in Table 3. As is generally known, LOI measures the minimum oxygen concentration of flowing gas mixed by oxygen and nitrogen required supporting downward flame combustion, which can be used as an indicator to evaluate the flammability characteristics of the epoxy thermosets. As the control samples, the DGEBA thermosets cured with three hardeners exhibit a low LOI around 22 vol.% due to their highly combustible natural. Owing to the long-term aggressive combustion with serious flaming drips, they also failed in the UL-94 vertical burning tests. It is prospective to find that the LOI values of the epoxy thermosets show a distinctive increase by incorporating PN–EPC, and furthermore, the increment of LOI is strongly dependent on the PN–EP content. When the content of PN–EPC was increased to 20 wt.%, the thermosets achieved a high LOI beyond 29 vol.%, which is fairly higher than the oxygen concentration of air. This means that these thermosets should almost be nonflammable in air, even if their LOI values varied a little when cured with different hardeners. On the other hand, the vertical burning experimental data listed in Table 3 also demonstrate that the UL-94 nonflammability rating of these epoxy thermosets was significantly improved in the presence of PN–EPC. When the content of PN–EPC was increased up to 15 wt.%, the cured thermosets achieved a V-1 rating, and moreover, the burned residues of these thermosets did not fall off during the vertical burning as a result of the good structural stability of all the thermosets. Such a feature seems to indicate the formation of a protective viscous char layer, which sticks to the surface of the thermoset instead of flowing away as it does for the conventional DGEBA thermosets. Nevertheless, the thermosets reached the V-0 rating when 20 wt.% of PN–EPC was added, which means these epoxy thermosets obtained an excellent nonflammability. It should be mentioned that most of the testing bars quenched within 6–8 s when flame agitator was removed during the vertical burning test, indicating an autoextinguishable feature.

It is noteworthy that the DGEBA/PN–EPC thermosets cured with DICY and DDM exhibit a better flame-retardant property than those with MeTHPA according to the LOI and UL-94 testing result. This phenomenon is ascribed to the contribution of nitrogen elements to the flame retardancy of thermosets when the nitrogen-containing hardeners are employed to cure with DGEBA/PN–EPC thermosetting systems. Moreover, the low crosslinking density resulting from the curing with MeTHPA also diminishes the flame retardancy of the thermosets. On the basis of the results as mentioned above, it is evident that the incorporation of PN–EPC can impart excellent flame retardancy to the conventional epoxy resin. Such a good flame-retardant property is attributed to the presence of unique combination of phosphorus and nitrogen in the thermosets as a result of chemically linking phosphazene rings to the backbone of epoxy resin in a covalent way. This characteristic molecular structure is highly advantageous to the reactive flame retardancy induced by the synergistic effect of phosphorus and nitrogen.

Table 3
The flame-retardant properties of the DGEBA/PN-EPC thermosets cured with three hardeners.

Thermoset sample	LOI value (vol.%)	Flammability from vertical burning testing			
		UL-94 classification	Flaming drips	Total flaming time (sec)	Maximal flaming time (sec)
DGEBA/DICY	22.7	Failed	Yes	> 250	> 50
DGEBA+5 wt.% PN-EPC[a]/DICY	25.2	Failed	None	201.6	47.3
DGEBA+10 wt.% PN-EPC[a]/DICY	26.7	V-1	None	136.8	25.5
DGEBA+15 wt.% PN-EPC[a]/DICY	29.1	V-1	None	45.8	12.6
DGEBA+20 wt.% PN-EPC[a]/DICY	31.8	V-0	None	23.1	6.7
DGEBA/DDM	22.5	Failed	Yes	> 250	> 50
DGEBA+5 wt.% PN-EPC[a]/DDM	24.9	Failed	None	205.2	44.2
DGEBA+10 wt.% PN-EPC[a]/DDM	26.2	V-1	None	127.9	29.2
DGEBA+15 wt.% PN-EPC[a]/DDM	28.7	V-1	None	55.8	14.7
DGEBA+20 wt.% PN-EPC[a]/DDM	31.2	V-0	None	22.7	6.4
DGEBA/MeTHPA	21.7	Failed	Yes	> 250	> 50
DGEBA+5 wt.% PN-EPC[a]/MeTHPA	24.6	Failed	Yes	208.6	42.1
DGEBA+10 wt.% PN-EPC[a]/MeTHPA	25.8	Failed	None	146.5	31.5
DGEBA+15 wt.% PN-EPC[a]/MeTHPA	28.1	V-1	None	52.5	15.4
DGEBA+20 wt.% PN-EPC[a]/MeTHPA	30.2	V-0	None	31.6	7.8

[a] The abbreviation of the cyclotriphosphazene-based epoxy compound.

Please cite this article in press as: Liu H, et al., Novel cyclotriphosphazene-based epoxy compound and its application in halogen-free epoxy thermosetting systems: Synthesis, curing behaviors, and flame retardancy, Polymer Degradation and Stability (2013), http://dx.doi.org/10.1016/j.polymdegradstab.2013.02.008

3.6. Investigation of flame-retardant mechanism

In order to visually recognize the effect of PN–EPC on the flammability characteristics of the epoxy thermosets, we recorded the total burning processes using digital camera from the simulated UL-94 vertical burning tests for some typical DGEBA/PN–EPC thermosets, and meanwhile, the combustion of the DGEBA thermoset as a control sample was also recorded. Fig. 13 shows the burning phenomena of these thermosets. It should be highly noted that, compared to the DGEBA thermosets exhibiting a highly combustible behavior, the epoxy thermoset did not present an aggressive combustion when 10 wt.% of PN–EPC was added. Additionally, the emission of few smoke and no flaming drips were observed for this sample during combustion. However, when 20 wt.% of PN–EPC was incorporated, one of the fascinating characteristics of combustion was observed that this thermoset just

Fig. 13. Digital photographs of the combustion procedures of (a) conventional DGEBA thermoset and DGEBA/PN–EPC thermosets containing (b) 5 wt.%, (c) 10 wt.%, (d) 15 wt.%, and (e) 20 wt.% of PN–EPC under a vertical burning condition.

Please cite this article in press as: Liu H, et al., Novel cyclotriphosphazene-based epoxy compound and its application in halogen-free epoxy thermosetting systems: Synthesis, curing behaviors, and flame retardancy, Polymer Degradation and Stability (2013), http://dx.doi.org/10.1016/j.polymdegradstab.2013.02.008

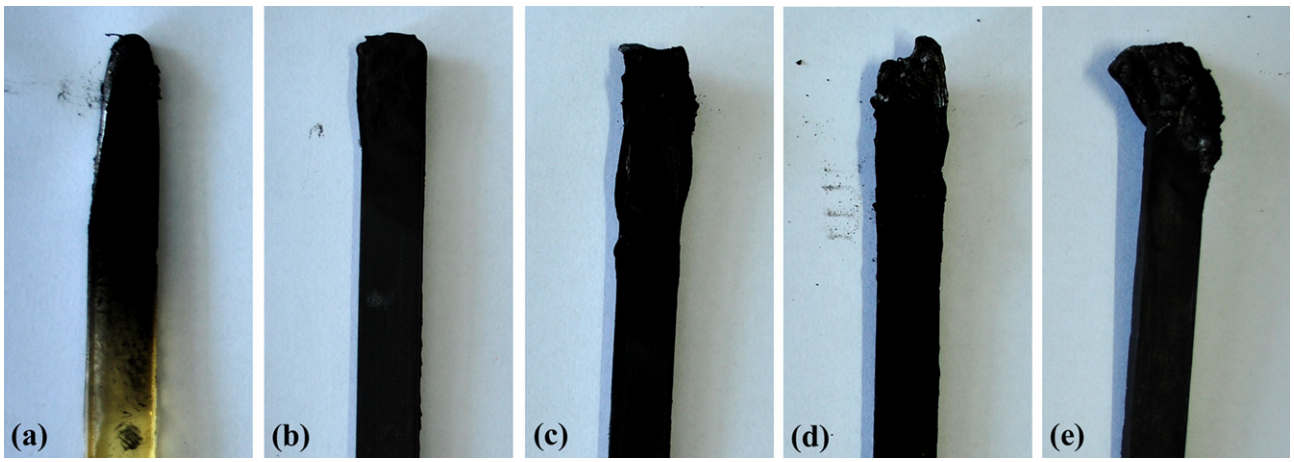

Fig. 14. Digital photographs of the test bars obtained from the vertical burning tests for (a) conventional DGEBA thermoset and DGEBA/PN–EPC thermosets containing (b) 5 wt.%, (c) 10 wt.%, (d) 15 wt.%, and (e) 20 wt.% of PN–EPC.

combusted slightly with a small blaze and was extinguished quickly by itself within 8 s after contacted by a flame for 10 s. It is interesting to observe that the surface of this thermoset has been covered with an expanded char layer by the end of combustion. This phenomenon implies that the char layer plays a critical roles in the fire resistance of the thermoset, and it serves as a protect layer for insulating the underlying material from heat source and preventing heat transfer and flame spread during combustion. These

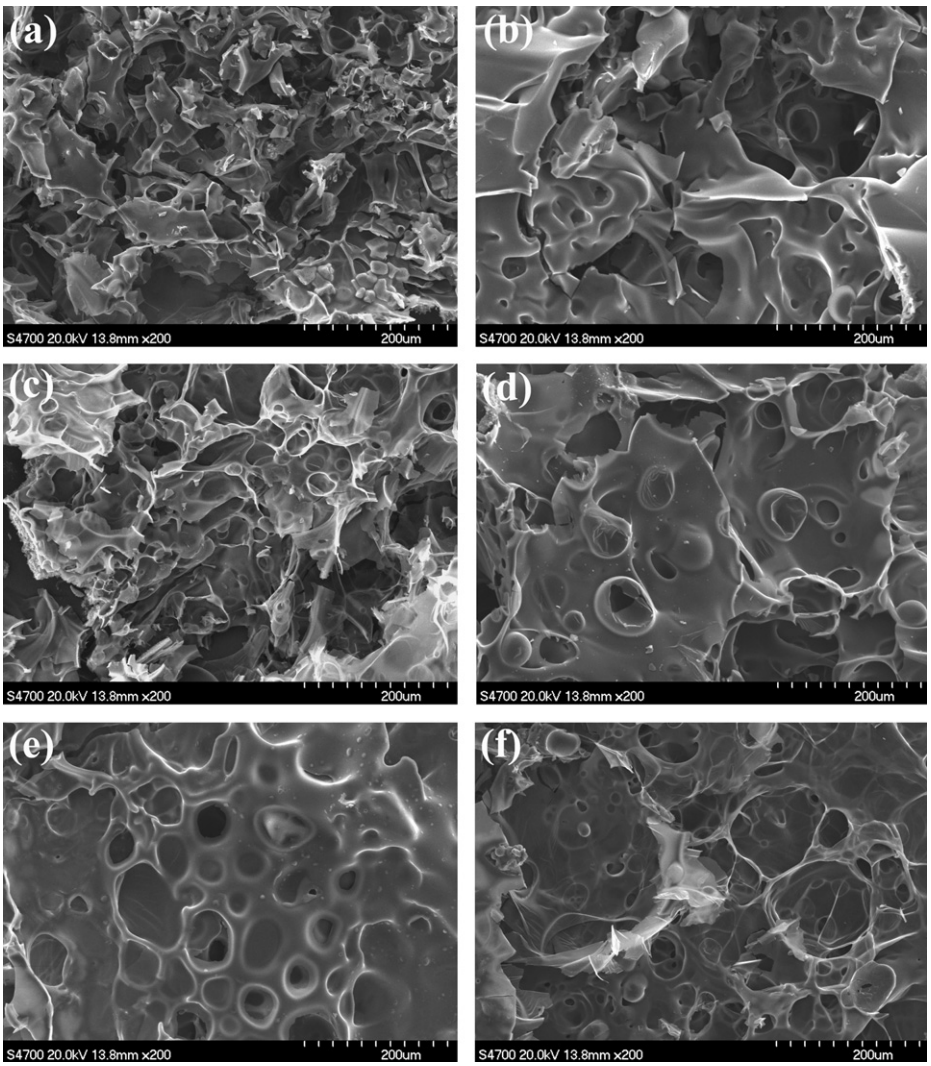

Fig. 15. SEM images of the residual chars collected from the tested bars after vertical burning tests for the thermosets containing (a) 5 wt.%, (b) 10 wt.%, (c) 15 wt.%, and (d) 20 wt.% of PN–EPC cured with DICY, (e) the thermosets containing 20 wt.% of PN–EPC cured with DDM, and (f) the thermosets containing 20 wt.% of PN–EPC cured with MeTHPA.

Please cite this article in press as: Liu H, et al., Novel cyclotriphosphazene-based epoxy compound and its application in halogen-free epoxy thermosetting systems: Synthesis, curing behaviors, and flame retardancy, Polymer Degradation and Stability (2013), http://dx.doi.org/10.1016/j.polymdegradstab.2013.02.008

photographs give a visible evidence of good flame retardancy for the DGEBA/PN–EPC thermosets.

Usually, the residual chars formed during combustion can give some important information for the inherent flammability characteristics of a polymeric material, and they can also reflect the flame-retardant mechanisms to some extent. Fig. 14 shows the profiles of the test bars of the epoxy thermosets after the UL-94 vertical burning tests, which demonstrates the status of the char formation after combustion. As seen in Fig. 14, there is almost no residue left after combustion for the DGEBA thermoset, and however, the surface of the residue obtained from the DGEBA/PN–EPC thermoset is covered with an expanded char layer. This suggests that the incorporation of PN–EPC into the DGEBA has generated a good intumescent effect. With increasing the content of PN–EPC, this intumescent effect becomes more significant. The morphology of these residual chars obtained from UL-94 vertical burning tests was investigated by SEM. Fig. 15 illustrates the SEM images of these residual chars. It is clearly observed that all the residual chars present a very gassy surface with a few pores breaking through, and the inside of the chars shows a honeycomb structure according to the magnified micrographs of each sample, indicating a typical morphology after the intumescent char formation. It is also notable that the perfection of the chars becomes better with increasing the content of PN–EPC, while the thermoset containing 5 wt.% of PN–EPC only exhibits some small irregular-shaped bulks. As is known, the physical structure of the charring layer usually plays a very important role in the performance of flame retardancy. From the observation of the residual chars of DGEBA/PN–EPC thermosets, the char layer formed during combustion is rigid and compact in nature, and there are lots of integrated closed honeycomb pores inside. Such a structural form favors the temperature grads in the char layer and protects the matrix inside. Therefore, it is assured that the cyclotriphosphazene moieties of PN–EPC can promote the formation of intumescent carbonaceous chars. Such a category of flame retarding mechanism is well known as “intumescent mechanism”. Following with this mechanism, an organic material can swell up when exposed to fire or heat to form a foamed mass, usually carbonaceous, which acts in the condensed phase promoting char formation on the surface as a barrier to inhibit gaseous products from diffusing to the flame and to shield the polymer surface from heat and air.

The chemical compositions of residual chars were further analyzed by FTIR spectroscopy. Fig. 16 shows the FTIR spectra of the residual chars collected from the three DGEBA/PN–EPC thermosets after UL-94 vertical burning tests. It seems that the three spectra present the similar patterns reflecting some highly carbonized compound, indicating these residual chars have a similar chemical structure. As seen in Fig. 16, a series of absorption peaks at 2364, 1631, 1504, and 1206 cm^{-1} can be attributed to the carbonized networks like aromatics and polyaromatics formed during the combustion. A broad absorption of P–O–P bond appears at around 1083 cm^{-1}, suggesting that the residual chars contain the polymerized phosphorus oxides. The appearance of P–O–P structure is considered as an evidence that such moieties are crosslinked to the other different species, resulting in the formation of a phosphorus-rich and complex-structured char [47,50]. A weak characteristic band at 2921 cm^{-1} is due to the organic part of the char and does not refer to the low content of the organic species in the char, because most of them have been strongly absorbed by the carbonized phosphorus-rich pyrolysis products. These results indicate that the residual chars mainly consist of cross-linked phosphoro-carbonaceous and phosphoro-oxidative solids as well as highly carbonized aromatic networks. In addition, the broad dual peaks are observed in the region of 3500–3000 cm^{-1}, which is attribute to the stretching vibration of O–H and N–H bonds. This indicates that the pyrolysis products of the thermosets include water and the other hydroxy compounds as well as the ammonium compounds.

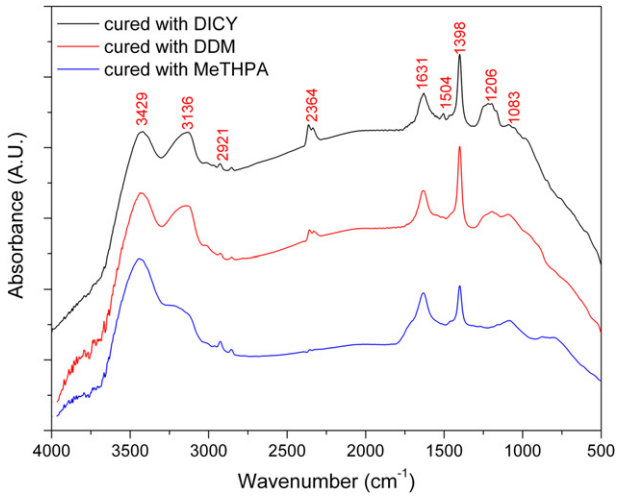

Fig. 16. FTIR spectra of the residual chars collected from the test bars of DGEBA/20 wt.% PN–EPC thermosets cured with three hardeners.

According to the investigation of the physical structure and chemical composition of residual chars, it can be deduced that the achievement of nonflammability of the DGEBA/PN–EPC thermosets results from the inherent flame retardancy of cyclotriphosphazene moieties due to its synergistic effect of phosphorus–nitrogen combination. Although the flame-retardant mechanism of phosphazene-based polymers like the complex epoxy thermosets prepared in this work is very complicated, it can be concluded that the presence of phosphazene rings chemically linking to the epoxy molecules enhances the flame retardancy in the ways of both condensed and gaseous phases [10,51,52]. The thermooxidative reaction of phosphazene rings with the other segments can form the intumescent and phosphorus-rich carbonaceous char on the surface as a barrier to prevent gaseous products from diffusing to the flame and to shield the polymer surface from heat and air during combustion. Meanwhile, the pyrolysis of phosphazene rings can produces phosphoric or polyphosphoric acid, which acts in the condensed phase promoting char formation. On the other hand, the cyclotriphosphazene moieties can release nonflammable gases such as CO_2, NH_3 and N_2 during combustion to dilute the hot atmosphere and cool the pyrolysis zone at the combustion surface. The aforementioned nonflammable gases can cut off the supply of oxygen, and thus leads to the autoextinguishability of the thermosets. Nevertheless, the effect of the molecular structures of phosphazene-based epoxy compounds and their participation in all stages of combustion process are not fully understood yet. A further intensive study is still necessary to clarify their effecting mechanisms, so that the optimal molecular structure of the phosphazene-based epoxy compound as a reactive-type flame retardant can be designed for the application to the nonflammable and high-performance epoxy thermosetting systems.

4. Conclusions

The novel cyclotriphosphazene-based epoxy compound, PN–EPC, was synthesized successfully in a good yield via a two-step synthetic route. The chemical structures and compositions of the intermediate and final products were confirmed by ^{1}H, ^{13}C, and ^{31}P NMR spectroscopy, FTIR spectroscopy elemental analysis, and mass

Please cite this article in press as: Liu H, et al., Novel cyclotriphosphazene-based epoxy compound and its application in halogen-free epoxy thermosetting systems: Synthesis, curing behaviors, and flame retardancy, Polymer Degradation and Stability (2013), http://dx.doi.org/10.1016/j.polymdegradstab.2013.02.008

spectroscopy. The curing kinetic parameters of the thermosetting systems consisting of DGEBA and PN–EPC with DICY, DDM, and MeTHPA as hardeners were determined by dynamic DSC scans under a nonisothermal condition. The incorporation of PN–EPC made the DGEBA thermosets achieve a significant improvement in T_g, and the resulting epoxy thermosets also obtained the good thermal stability with a high char yield. Owing to the unique combination of phosphorus and nitrogen induced from the phosphazene rings, the incorporation of PN–EPC imparted an excellent nonflammability to the resulting epoxy thermosets by a synergistic effect on flame retardancy. As a result, these epoxy thermosets achieved high LOI values and UL-94 V-0 rating when 20 wt.% of PN–EPC was added. The investigation on the flame-retardant mechanisms suggested that the pyrolysis products of phosphazene rings acted in both the condensed and gaseous phases to promote the formation of intumescent phosphorus-rich char on the surface of thermosets. Such a char layer can supply a much better barrier for underlying the thermosets to inhibit gaseous products from diffusing to the flame, to shield the material surface from heat and air, and to prevent or slow down oxygen diffusion. As a non-halogenated reactive-type flame retardant, the PN–EPC synthesized in this study can ensure a greater safety and excellent flame retardancy for the fire-resistant applications in the epoxy thermosetting systems.

Acknowledgment

The financial support from the National Natural Science Foundation of China (Project Grant No.: 50973005, 51173010) is gratefully acknowledged.

References

[1] Wan J, Li C, Bu Z, Xu C, Li B, Fan H. A comparative study of epoxy resin cured with a linear diamine and a branched polyamine. Chem Eng J 2012;188:160–72.
[2] Nakamura Y, Yamaguchi M, Okubo M, Matsumoto T. Effects of particle size on mechanical and impact properties of epoxy resin filled with spherical silica. J Appl Polym Sci 1992;45(7):1281–9.
[3] Gu J, Zhang G, Dong S, Zhang Q, Kong J. Study on preparation and fire-retardant mechanism analysis of intumescent flame-retardant coatings. Surf Coat Technol 2007;201(18):7835–41.
[4] Sun D, Yao Y. Synthesis of three novel phosphorus-containing flame retardants and their application in epoxy resins. Polym Degrad Stab 2011;96(10):1720–4.
[5] Uddin MA, Bhaskar T, Kusaba T, Hamano K, Muto A, Sakata Y. Debromination of flame retardant high impact polystyrene (HIPS–Br) by hydrothermal treatment and recovery of bromine free plastics. Green Chem 2003;5(2):260–3.
[6] Pecht M, Deng Y. Electronic device encapsulation using red phosphorus flame retardants. Microelectron Reliab 2006;46(1):53–62.
[7] Liu J, Tang J, Wang X, Wu D. Synthesis, characterization and curing properties of a novel cyclolinear phosphazene-based epoxy resin for halogen-free flame retardancy and high performance. RSC Adv 2012;2:5789–99.
[8] Bras ML, Wilkie CA, Bourbigot S. Fire retardancy of polymers: new applications of mineral fillers. Cambridge: The Royal Society of Chemistry; 2005. p. 126.
[9] Wang G, Cheng W, Tu Y, Wang C, Chen C. Characterizations of a new flame-retardant polymer. Polym Degrad Stab 2006;91(12):3344–53.
[10] Laoutid F, Bonnaud L, Alexandre M, Lopez-Cuesta J, Dubois P. New prospects in flame retardant polymer materials: from fundamentals to nanocomposites. Mater Sci Eng R 2009;63(3):100–25.
[11] Lu S, Hamerton I. Recent developments in the chemistry of halogen-free flame retardant polymers. Prog Polym Sci 2002;27(8):1661–712.
[12] Gouri ME, Bachiri AE, Hegazi SE, Rafik M, Harfi AE. Thermal degradation of a reactive flame retardant based on cyclotriphosphazene and its blend with DGEBA epoxy resin. Polym Degrad Stab 2009;94(11):2101–6.
[13] Kang N, Du Z, Li H, Zhang C. Synthesis and characterization of P/Si flame retardant and its application in epoxy systems. Polym Adv Technol 2013;23(10):1329–34.
[14] Cyriac A, Lee SH, Varghese JK, Park JH, Jeon JY, Kim SJ, et al. Preparation of flame-retarding poly(propylene carbonate). Green Chem 2011;13(12):3469–75.
[15] Lin YL, Hsiue GH, Lee RH, Chiu YS. Phosphorus-containing epoxy for flame retardant. III: using phosphorylated diamines as curing agents. J Appl Polym Sci 1997;63(7):895–901.
[16] Toldy A, Toth N, Anna P, Marosi G. Synthesis of phosphorus-based flame retardant systems and their use in a epoxy resin. Polym Degrad Stab 2006;91(3):585–92.
[17] Wang X, Song L, Xing W, Lu H, Hu Y. A effective flame retardant for epoxy resins based on poly(DOPO substituted dihydroxyl phenyl pentaerythritol diphosphonate). Mater Chem Phys 2011;125(3):536–41.
[18] Gao F, Tong L, Fang Z. Effect of a novel phosphorous–nitrogen containing intumescent flame retardant on the fire retardancy and the thermal behaviour of poly(butylene terephthalate). Polym Degrad Stab 2006;91(6):1295–9.
[19] Sun S, He Y, Wang X, Wu D. Flammability characteristics and performance of halogen-free flame-retarded polyoxymethylene based on phosphorus–nitrogen synergistic effects. J Appl Polym Sci 2010;118(1):611–22.
[20] Shieh JY, Wang CS. Effect of the organophosphate structure on the physical and flame-retardant properties of an epoxy resin. J Polym Sci Part A: Polym Chem 2002;40(3):369–78.
[21] Gao L, Wang D, Wang Y, Wang J, Yang B. A flame-retardant epoxy resin based on a reactive phosphorus-containing monomer of DODPP and its thermal and flame-retardant properties. Polym Degrad Stab 2008;93(7):1308–15.
[22] Schartel B, Braun U, Artner J, Ciesielski M, Doring M, Altstadt V. Pyrolysis and fire behavior of epoxy systems containing a novel 9, 10–dihydro–9–cxa–10–phosphaphenanthrene–10–oxide– (DOPO) –based diamino hardener. Eur Polym J 2008;44(3):704–15.
[23] Ren H, Sun J, Wu B, Zhou Q. Synthesis and properties of a phosphorus-containing flame retardant epoxy resin based on bis-phenoxy (3-hydroxy) phenyl phosphine oxide. Polym Degrad Stab 2007;92(6):956–61.
[24] Chen H, Zhang Y, Chen L, Shao Z, Liu Y, Wang Y. Novel inherently flame-retardant poly(trimethylene terephthalate) copolyester with the phosphorus-containing linking pendent group. Ind Eng Chem Res 2010;49(15):7052–9.
[25] Jeng RJ, Shau M, Lin JJ, Su WC, Chiu YS. Flame retardant epoxy polymers based on all phosphorus-containing components. Eur Polym J 2002;38(4):683–93.
[26] Kandola BK, Biswas B, Price D, Horrocks AR. Studies on the effect of different levels of toughener and flame retardants on thermal stability of epoxy resin. Polym Degrad Stab 2010;95(2):144–52.
[27] Chandrasekhar V, Krishnan V. Advances in the chemistry of chlorocyclophospazenes. Adv Inorg Chem 2002;53:159–211.
[28] Liu R, Wang X. Synthesis, characterization, thermal properties and flame retardancy of novel nonflammable phosphazene-based epoxy resin. Polym Degrad Stab 2009;94(4):617–24.
[29] Chen-Yang YW, Yuan CY, Li CH, Yang HC. Preparation and characterization of novel flame retardant (aliphatic phosphate)cyclotriphosphazene-containing polyurethanes. J Appl Polym Sci 2003;90(5):1357–64.
[30] Diefenbach D, Allcock HR. Synthesis of cyclo- and polyphosphazenes with pyridine side groups. Inorg Chem 1994;33(20):4562–5.
[31] Jaeger RD, Gleria M. Poly(organophosphazene)s and related compounds: synthesis, properties and applications. Prog Polym Sci 1998;23(2):179–276.
[32] Allcock HR. New approaches to hybrid polymers that contain phosphazene rings. J Inorg Organomet Polym Mater 2007;17(2):349–59.
[33] Chang JY, Rhee SB, Cheong S, Yoon M. Synthesis and thermal reaction of acetylenic group substituted poly(organophosphazenes) and cyclotriphosphazene. Macromolecules 1992;25(10):2666–70.
[34] Allcock HR, Austin PE. Schiff base coupling of cyclic and high-polymeric phosphazenes to aldehydes and amines: chemotherapeutic models. Macromolecules 1981;14(6):1616–22.
[35] Chen-Yang YW, Cheng SJ, Tsai BD. Preparation of the partially substituted(phenoxy) chlorocyclotriphosphazenes by phase-transfer catalysis. Ind Eng Chem Res 1991;30(6):1314–9.
[36] Ding J, Shi W. Thermal degradation and flame retardancy of hexaacrylated/hexaethoxyl cyclophosphazene and their blends with epoxy acrylate. Polym Degrad Stab 2004;84(1):159–65.
[37] Allcock HR. A perspective of polyphosphazene research. J Inorg Organomet Polym Mater 2006;16(4):277–94.
[38] Menczel JD, Prime RB. Thermal analysis of polymers: fundamentals and applications. Hoboken: John Wiley & Sons; 2009.
[39] Haines PJ. Principles of thermal analysis and calorimetry. Cambridge: The Royal Society of Chemistry; 2002.
[40] He YS, Zeng JB, Li SL, Wang YZ. Crystallization behavior of partially miscible biodegradable poly(butylene succinate)/poly(ethylene succinate) blends. Thermochim Acta 2012;529:80–6.
[41] Sbirrazzuoli N, Vyazovkin S, Mititelu A, Sladic C, Vicent L. A study of epoxy-amine cure kinetics by combining isoconversional analysis with temperature modulated DSC and dynamic rheometry. Macromol Chem Phys 2003;204(15):1815–21.
[42] Kissinger HE. Reaction kinetics in differential thermal analysis. Anal Chem 1957;29(11):1702–6.
[43] Ozawa T. A new method of analyzing thermogravimetric data. Bull Chem Soc Jpn 1965;38(11):1881–6.
[44] Liu W, Qiu Q, Wang J, Huo Z, Sun H. Curing kinetics and properties of epoxy resin-fluorenyl diamine systems. Polymer 2008;49(20):4399–405.
[45] Rane LW, Dynes PJ, Kaelble DH. Analysis of curing kinetics in polymer composites. J Polym Sci Polym Lett Ed 1973;11(8):533–40.

Please cite this article in press as: Liu H, et al., Novel cyclotriphosphazene-based epoxy compound and its application in halogen-free epoxy thermosetting systems: Synthesis, curing behaviors, and flame retardancy, Polymer Degradation and Stability (2013), http://dx.doi.org/10.1016/j.polymdegradstab.2013.02.008

[46] Jubsilp C, Damrongsakkul S, Takeichi T, Rimdusit S. Curing kinetics of arylamine-based polyfunctional benzoxazine resins by dynamic differential scanning calorimetry. Thermochim Acta 2006;477(2):131–40.
[47] Zhu SW, Shi WF. Thermal degradation of a new flame retardant phosphate methacrylate polymer. Polym Degrad Stab 2003;80(2):217–22.
[48] Devapal D, Packirisamy S, Reghunadhan Nair CP, Ninan KN. Phosphazene-based polymers as atomic oxygen resistant materials. J Mater Sci 2006;41(17):5764–6.
[49] Allcock HR, Taylor JP. Phosphorylation of phosphazenes and its effects on thermal properties and fire retardant behavior. Polym Eng Sci 2000;40(5):1177–89.
[50] Gouri ME, Bachiri AE, Hegazi SE, Ziraoui R, Rafik M, Harfi AE. A phosphazene compound multipurpose application–composite material precursor and reactive flame retardant for epoxy resin materials. J Mater Environ Sci 2011;2(4):319–34.
[51] Nie S, Hu Y, Song L, He Q, Yang D, Chen H. Synergistic effect between a char forming agent (CFA) and microencapsulated ammonium polyphosphate on the thermal and flame retardant properties of polypropylene. Polym Adv Technol 2008;19(8):1077–83.
[52] Levchik SV, Weil ED. A review of recent progress in phosphorus-based flame retardants. J Fire Sci 2006;24(5):345–64.

Please cite this article in press as: Liu H, et al., Novel cyclotriphosphazene-based epoxy compound and its application in halogen-free epoxy thermosetting systems: Synthesis, curing behaviors, and flame retardancy, Polymer Degradation and Stability (2013), http://dx.doi.org/10.1016/j.polymdegradstab.2013.02.008